Bottom water redox dynamics during the Early Cretaceous Weissert Event in ODP Hole 692B (Weddell Sea, Antarctica) reconstructed from the benthic foraminiferal assemblages

Victor M. Giraldo-Gómez[a*], Maria Rose Petrizzo[a], Cinzia Bottini[a], Carla Möller[a,c], Thomas Wagner[b], Liyenne Cavalheiro[a,b], Onoriode Esegbue[b,e], Gabriele Gambacorta[d], Elisabetta Erba[a].

[a]Università degli Studi di Milano, Dipartimento di Scienze della Terra "Ardito Desio", Via Mangiagalli 34, 20133 Milano, Italy.

[b]Lyell Centre, Heriot-Watt University, EH14 4AP, Edinburgh, UK.

[c]Ruhr - University Bochum, Institute for Geology, Mineralogy and Geophysics, Universitätsstraße 150, 44801 Bochum, Germany.

[d]Eni S.p.A. Natural Resources - Geology and Geophysics Research and Technological Innovation, Milan, Italy.

[e]Newcastle University, School of Natural and Environmental Sciences, NE1 7RU, Newcastle upon Tyne, UK.

[*]Corresponding author.

E-mail addresses: victor.giraldo@unimi.it (Victor M. Giraldo-Gómez), mrose.petrizzo@unimi.it (Maria Rose Petrizzo), cinzia.bottini@unimi.it (Cinzia Bottini), carla.moeller@rub.de (Carla Möller), t.wagner@hw.ac.uk (Thomas Wagner), liyenne.cavalheiro@unimi.it (Liyenne Cavalheiro), onoriode.esegbue@newcastle.ac.uk (Onoriode Esegbue), gabriele.gambacorta@eni.com (Gabriele Gambacorta), elisabetta.erba@unimi.it (Elisabetta Erba).

Keywords: Benthic foraminifera; Early Cretaceous; Weissert Event; bottom-water redox;

paleoceanography; Antarctica.

Abstract

Benthic foraminifera at Ocean Drilling Program (ODP) Hole 692B were studied to understand variations in oxygen and organic-matter fluxes in bottom waters during the Early Cretaceous. The upper Berriasian to lower Barremian black shales, characterized by high concentrations of total organic carbon (TOC) ranging between 1.3 and 18%, were deposited in an outer neritic-upper bathyal environment (~200 - 500 m) according to benthic foraminifera assemblages. A new high-resolution record of benthic foraminiferal assemblages of high-latitude, dominated by infaunal taxa (*Citharina, Eoguttulina, Laevidentalina, Lagena, Lenticulina, Marginulina, N*odosaria*, Planularia, Saracenaria,* and *Vaginulinopsis*), is described in depleted-oxygen and high organic-carbon flux conditions.

Extremely dysoxic conditions are recorded at the onset of the carbon isotope excursion (CIE) during the Weissert Event (upper Valanginian), followed by a period of anoxic conditions in bottom waters. A repopulation event of benthic foraminifera, linked to an increase in oxygen concentrations, coincided with the global cooling episode, marking the late part of the Weissert Event and indicating a significant disturbance in bottom waters.

Subsequently, there were short periods in the upper Valanginian and the uppermost lower Hauterivian where the bottom waters experienced an increased oxygen concentration. Possibly, bottom currents owing to the influx of Southern Ocean waters favored short-term pulses of ventilation under constant increased organic-carbon flux during the upper Valanginian and upper Hauterivian.

1. Introduction

The Early Cretaceous represents a greenhouse period with phases of high atmospheric CO_2 concentrations and high global mean temperatures (Royer et al., 2007; Littler et al., 2011). However,

multiproxy studies (e.g., Weissert and Erba, 2004; O'Brien et al., 2017; Bottini and Erba, 2018) have shown significant climate variability associated with global oceanic anoxic events (OAEs), the emplacement of large igneous provinces and the opening or closure of oceanic gateways.

As evidenced by different proxies, the response of the biota unravels the changes in disturbed and stable environments of the oceanic biosphere. Records from high paleolatitudes and restricted basins are of particular relevance, as they provide new evidence about biotic reactions to regional and global changes.

During the Cretaceous, the accumulation of organic-rich strata (black shale) was recorded both in epicontinental seas and oceanic basins (Arthur and Sageman, 1994), and was used to define Oceanic Anoxic Events (OAEs) that implied oxygen-depletion of intermediate and bottom-waters, promoting enhanced burial of organic matter on a global scale (Schlanger and Jenkyns, 1976; Arthur and Schlanger, 1979; Arthur et al., 1990). During the Valanginian, a major environmental change is evidenced from a positive $\delta^{13}C$ excursion (CIE) named the Weissert Event by Erba et al. (2004). The event was associated with multiple climatic and paleoceanographic changes (e.g., Weissert 1989; Erba et al., 2004; Westermann et al., 2010; Meissnner et al., 2015), which probably were triggered by volcanic activity of the Paraná-Etendeka Large Igneous Province (LIP) (Erba et al., 2004, 2019; Weissert and Erba, 2004; Sprovieri et al., 2006; Thiede and Vasconcelos, 2010; Gréselle et al., 2011; Martinez et al., 2015).

In this study, we analyze benthic foraminiferal assemblages in the upper Berriasian - lower Barremian section recovered at Ocean Drilling Program (ODP) Hole 692B drilled in the Weddell Sea (Fig. 1), intending to characterize the paleoceanographic changes that occurred in a basin formed during the initial separation of Antarctica from Gondwana. During the Early Cretaceous, Antarctica was the centerpiece of a large landmass extending from South America across the southern latitudes to Australasia (Zinsmeister, 1986). From Hauterivian times, an incipient separation began between Antarctica and Madagascar-India, which finished during the mid-Cretaceous (Wilford and Brown, 1994).

Meanwhile, the Southern Ocean (Atlantic and SW Indian oceans) was characterized by extensive continental shelves and deeper basins (Fig. 1).

Benthic foraminifera in ODP Hole 692B were described by the Shipboard Scientific Party of ODP Leg 113 (Barker et al., 1988), in which a few analyzed samples were interpreted to be characterized by low levels of bottom water oxygen in a middle bathyal (500-1000 m) paleobathymetric setting (Barker et al., 1988).

We conducted a high-resolution study of the benthic foraminiferal assemblages of the upper Berriasian to lower Barremian interval integrated with stable carbon isotope and total organic carbon data. For that, we used a revised chronostratigraphic framework based on calcareous nannofossil biostratigraphy. (Cavalheiro et al., 2021). The primary aims of this study are the identification of: 1) quantitative changes in benthic foraminiferal assemblages to derive oxygen and organic-matter fluxes to the seafloor; 2) the paleobathymetric setting; 3) the paleoecological preferences of benthic foraminifera; and thus, paleoenvironmental changes in bottom water conditions before, during and after the Weissert Event.

2. Material and methods

2.1 ODP Hole 692B

ODP Hole 692B is located in the Weddell Sea (70°43.432'S, 13°49.195'W, East Antarctica) at water depth of 2875 m (Figs. 1A, 1B) and was cored for a total length of 97.9 m with only 30% (29.3 m) of sediment recovery due to operational problems (Barker et al., 1988).

Cretaceous sedimentary rocks corresponding to Unit III (cores 113-692B-7R to 113-692B-12R; Barker et al., 1988) are characterized from top to bottom (Fig. 2) by common claystone (core 113-692B-7R), mixed sedimentary rocks composed of ash and nannofossil-bearing claystone, organic and nannofossil-bearing mudstone, organic-bearing muddy nannofossil chalk, carbonate-bearing nannofossil

claystone and mudstone (cores 113-692B-8R to 113-692B-10R), and carbonate-bearing and nannofossil-bearing clayey mudstone (core 113-692B-12R). Moreover, volcanic beds, layers, and lenses with a high percentage of carbonate are recorded commonly through Unit III (Barker et al., 1988).

2.2 Calcareous nannofossils

A total of 112 samples were examined for calcareous nannofossil biostratigraphy in the interval between 93 mbsf (meters below seafloor) (sample113-692B-12R, CC) and 53.53 mbsf (sample113-692B-7R-1, 32 cm) (see Supplementary data, Table S1). Samples were prepared using a simple smear slide technique: a small piece of rock was powdered, adding a few drops of bi-distillate water without centrifuging, ultrasonic cleaning, or settling the sediment, thus retaining the original rock composition. Investigations were performed with a polarizing light microscope at 1250 X magnification. Since calcareous nannofossil assemblages in ODP Hole 692B include a combination of high latitude taxa, cosmopolitan species, and a few Tethyan species (Mutterlose and Wise, 1990), biostratigraphy has been derived regarding standard zonation schemes for the Boreal Realm (BC zonation after Bown et al., 1998) and the Tethys Ocean (NC zonation after Bralower et al., 1995).

2.3 Geochemistry ($\delta^{13}C_{org}$ and TOC)

A total of 143 samples, including a published data set (Cavalheiro et al., 2021), were analyzed for bulk organic stable carbon isotope ratios ($\delta^{13}C_{org}$) by Europa Scientific Elemental Analyser - Isotope Ratio Mass Spectrometry (EA - IRMS). Analysis was carried out at Iso-Analytical, Crewe Cheshire (UK). Measurements of the TOC content of 67 samples were also carried out along with $\delta^{13}C_{org}$ analysis. Repeated analysis on reference materials (e.g., IAEA-CH-6, IA-R001, IA-R005 and IA-R006) and duplicate sample measurements yielded a standard deviation < 0.1. Carbon isotope and TOC results are reported in the standard Vienna Pee Dee Bee δ notation (VPDB) and weight percentage (%), respectively.

2.4 Benthic foraminifera

A total of 69 samples (from samples 113-692B-7R-1, 42-45 cm to 113-692B-12R-3, 112-115 cm; Supplementary data, Table S2) of about 3-17 g in weight (an average of 7 g/sample) were processed to obtain washed residues using hydrogen peroxide (H_2O_2). Samples were washed under tap water through different sieves (meshes of 355 μm, 250 μm, 125 μm, and 63 μm). Because of the small size of the samples, all residues of the size-fractions > 63 μm were picked for benthic foraminifera (BF) and, when possible, at least 200 specimens were picked, identified, counted, and permanently stored in Plummer slides. The abundance of radiolaria, calcispheres, and pyrite observed in the washed residues are reported in Supplementary data, Table S2.

Benthic foraminiferal numbers (BFN) were calculated for the >63 μm size fraction as specimens per 10 g of dry sediment (n/10g). Based on the counts of BF, three faunal indices were calculated for all samples as follows: 1) species richness (S), which is the number of different species in a community, 2) dominance (D) is the degree to which a taxon is more or less abundant in a community (Abundant: D=0; scarce: D=1), and 3) Shannon diversity index (H_S) that measures the heterogeneity of a population, taking into account the evenness of species abundances (Shannon and Weaver, 1949).

Statistical analyses were applied using the PAST software 3.1 (Hammer et al., 2001). A non-metric multidimensional scaling (NMDS; Q-mode) and a detrended correspondence analysis (DCA; R-mode) were performed on the abundance data of benthic foraminifera to reconstruct environmental changes. The NMDS and DCA are based on the Bray-Curtis similarity index (in two dimensions - samples) and the Pearson correlation (in two dimensions - taxa), respectively.

Taxa were subdivided into morphogroups according to their ecological preferences, specifically infaunal and epifaunal (e.g., Koutsoukos, 1989; Murray, 1991; Jorissen et al., 2007). Although some opportunistic foraminifera are characterized by their high adaptive capacity to live on top (epifauna) or within (infauna) of the uppermost centimeter of the sediment (e.g., Koutsoukos, 1989; Kaminski et al.,

1995; Erbacher et al., 1998; Holbourn et al., 2001b; Friedrich et al., 2003, 2009), we have inferred in this study that most of the benthic foraminifera assemblages are dominated by taxa with infaunal preferences.

The marker species, BFN, H_S and D were used to reconstruct the oxygen availability and increases/decreases in organic carbon fluxes in bottom waters (e.g., Koutsoukos, 1989; Jorissen et al., 1995; van der Zwaan et al., 1999; Holbourn et al., 2001b; Friedrich et al., 2003, Friedrich and Hemleben, 2007).

The paleo-bathymetric subdivisions used in this study are according to Nyong and Olsson (1984) and van Morkhoven et al. (1986). They are inner-neritic (IN: 0 - 50 m), middle-neritic (MN: 50 - 100 m), outer-neritic (ON: 100 - 200 m), upper bathyal (UB: 200 - 500 m), middle bathyal (MB: 500 - 1000 m), and lower bathyal (LB: 1000 - 2000 m). The bottom water-oxygenation has been evaluated as anoxic (without detectable oxygen concentration) and dysoxic (with some oxygen concentration) following Jorissen et al. (2007). The dysoxic conditions were subdivided into three categories, according to the increase and decrease of the abundances (BFN) and diversity indices (H_S and D) of benthic foraminifera, allowing interpretation of the oxygen availability in the bottom waters as follows: extremely dysoxic (low BFN and H_S, high D), severely dysoxic (low BFN and H_S, moderate D) and moderately dysoxic (high BFN and H_S, moderate to low D). For this interpretation, we identify a range of values for each variable (BFN, H_S, and D) to constrain the categories (low, moderate, and high) as follow: BFN (minimum value: 1 specimen - maximum value: 500 specimens): low values: 1-166 specimens; moderate values: 167-333 specimens; high values: 334-500 specimens; H_S (minimum value: 0 - maximum value: 3): low values: 0-1; moderate values: 1-2; high values: 2-3; D (minimum value: 0 - maximum value: 1): low values: 0-0.33; moderate values: 0.34-0.66; high values: 0.67-1.

The most important taxa identified in ODP Hole 692B were photographed using the Scanning Electron Microscopy (SEM - Jeol JSM-IT500) at the Department of Earth Sciences “A. Desio” of the Università degli Studi di Milano.

3. Results

3.1 Calcareous nannofossil biostratigraphy

The new calcareous nannofossil biostratigraphy of ODP Hole 692B allowed a revision of the age assignment by Mutterlose and Wise (1990) for the stratigraphic interval comprised between 93 mbsf and 53.53 mbsf, initially interpreted to be Valanginian- Hauterivian. The revised calcareous nannofossil biostratigraphy applies the chronostratigraphic framework of the Berriasian - Barremian interval reported in Cavalheiro et al. (2021). Calcareous nannofossil assemblages (Supplementary Fig S1, Table S1) contain relatively diverse and moderate to well-preserved specimens. The nannoflora is dominated by a few species, most prominently *Watznaueria barnesiae*, and in the interval between 91.87 mbsf (sample 113-692B-12R-3, 65-68 cm) and 80.52 mbsf (sample 113-692B-10R-2, 50-54 cm), *Biscutum constans* and *Crucibiscutum salebrosum.* A few barren samples were detected in core 12R (91.31, 90.57, 90.42, 89.4, 89.22, 88.93, 88.78 and 88.50 mbsf), in core 8R (59.67 mbsf) and in core 7R (55.23, 54.31, 53.87, and 53.2 mbsf). The topmost part of the investigated section, from 61.91 mbsf (113-692B-8R-2, 12-14 cm) to 53.2 mbsf, is characterized by poorly preserved and scarce nannofossils (Fig. 2).

The lowermost studied sample at 93 mbsf (sample 113-692B-12R-CC) is not older than late Berriasian and corresponds to Zone BC2 *(*Bown et al., 1998) and subzone NC2b (Bralower et al., 1995) is characterized by the presence of the boreal taxon *Crucibiscutum ryazanicum* and the Tethyan taxon *Percivalia fenestrata*.

The interval 93-91.87 mbsf (sample 113-692B-12R-3, 65-68 cm) is attributed to the late Berriasian - early Valanginian (Zones BC2-BC3 and NC2b). A more precise age assignment of this interval is not possible due to the absence of Boreal (i.e. *Triquetrorhabdulus shetlandensis* and *Michrantolithus speetonensis*) and Tethyan (i.e. *Calcicalathina oblongata*) marker species for the base of the Valanginian. The first occurrence (FO) of *Zeugrhabdotus trivectis* at 91.87 mbsf that shortly precedes the onset of the positive $\delta^{13}C$ isotopic excursion of the Weissert Event was also identified in worldwide sections (Kessels

et al., 2006; Duchamp-Alphonse et al., 2007; Barbarin et al., 2012; Charbonnier et al., 2013; Aguado et al., 2018; see Cavalheiro et al., 2021 for further discussion) and indicates subzone NC3a and Zone BC4.

The base of subzone NC3b is identified at the last occurrence (LO) of *Rucinolithus wisei* detected at 89.02 mbsf (sample 113-692B-12R-1, 80-83 cm), suggestive of a late Valanginian age. In ODP Hole 692B, the LO of *R. wisei* correlates with the early phase of the Weissert Event similarly to other records worldwide (SE France: Duchamp et al., 2007, Charbonnier et al., 2013; Central Atlantic: Bornemann and Mutterlose, 2008; and SE Spain: Aguado et al., 2018).

Disarticulated elements of possible *Micrantholithus speetonensis* were found in ODP Hole 692B in the interval between 84.03 mbsf (sample 113-692B-10R-4, 101-104 cm) and 83.74 mbsf (sample 113-692B-10R-4, 73-75 cm) in correspondence with the topmost part of the CIE. This finding is consistent with the recent revision of the LO of *M. speetonensis,* placed in the late Valanginian, close to the topmost part of the Weissert Event (Möller et al., 2015). The LO of *M. speetonenesi* marks the base of Zone BC5 and the NC3/NC4 zonal boundary is tentatively placed between 82 mbsf and 83 mbsf just above the CIE of the Weissert Event following the inter-calibration of *Tubodiscus verenae* (absent in ODP Hole 692B) concerning the chemo- and magneto-stratigraphy (see Cavalheiro et al., 2021 for further discussion).

The absence of low and high latitude markers such as *Tubodiscus verenae* (Bralower et al., 1995) and *Triquetrorhabdulus shetlandensis* and/or *Eprolithus antiquus* (Bown et al., 1998), respectively, makes the identification of the Valanginian/Hauterivian boundary not straightforward in ODP Hole 692B. Since in the literature, the last common occurrence (LCO) of *Cyclagelosphaera deflandrei* was documented in the latest Valanginian after the LO of *T. verenae,* within subzone NC4a and close to the Valanginian/Hauterivian boundary (Roth, 1983; Thierstein, 1976; Erba and Quadrio, 1987), the Valanginian/Hauterivian boundary is here constrained using the LCO of *C. deflandrei* detected at 80.98 mbsf (sample 113-692B-10R-2, 96-99 cm). Moreover, in ODP Hole 692B, the LCO of *C. deflandrei* is

above the CIE of the Weissert Event, thus, in the equivalent stratigraphic position reported in several works (e.g., Channell et al., 1993; Roth, 1983; Littler et al., 2011; Applegate and Bergen, 1988; Kessels et al., 2006).

The FO of *Tranolithus octiformis* at 72.10 mbsf (sample 113-692B-9R-3, 29-31 cm) marks the base of Zone BC8 (Bown et al., 1998). This event is shortly followed by the FO of *Rucinolithus terebrodentarius* at 71.24 mbsf (sample 113-692B-9R-2, 92-95cm), which defines the base of subzone NC5b (Bralower et al., 1995), indicating a late Hauterivian age (Supplementary Fig. S1).

A distinctive change in the nannofossil assemblage composition is detected at 70.59 mbsf (sample 113-692B-9R-2, 27-30 cm): *C. salebrosum* is no longer present, while *Cyclagelosphaera margerelii* is frequent-common and, from 69.28 mbsf upwards (sample 113-692B-9R-1, 47-49 cm), *Watznaueria britannica* is also frequent. *Diazomatolithus lehmanii* is present up to 62.32 mbsf (sample 113-692B-8R-3, 1-3 cm), where its LCO is detected (Supplementary Fig. S1). In the biozonation of Bown et al. (1998) and boreal records (Jeremiah, 2001), abundant *C. margerelii* is recorded in the late early Barremian within Zones BC13 and BC14, together with relatively frequent *W. britannica* (Bown et al., 1998; Jeremiah, 2001). The LCO of *D. lehmanii* is reported in Zone BC15 (Bown et al., 1998; Jeremiah, 2001).

We, therefore, interpret the nannofloral assemblages detected in ODP Hole 692B between 70.59 and 62.32 mbsf to correspond to Zones BC13 - BC15 of Bown et al. (1998). In the same interval, low latitude marker species are absent, and thus the identification of Zones NC5b to NC5d (Bralower et al., 1995) was based on the Boreal-Tethyan correlation of Bown et al. (1998). The sharp change in nannofossil assemblages and the marked thin thickness of the upper Hauterivian stratigraphic interval suggest a hiatus at 70.59 mbsf, probably eliding part of the late Hauterivian. Samples from 61.91 mbsf to the top of the studied interval are barren of nannofossils or contain very rare *W. barnesiae* specimens, making the age determination impossible.

3.2. $\delta^{13}C_{org}$ and TOC

$\delta^{13}C_{org}$ values recorded in ODP Hole 692B range between -31.9 and -28.7‰ (from sample 113-692B-12R-3, 112-115 cm to 113-692B-7R-1, 42-45 cm, 92.34 to 53.65 mbsf in Fig. 2). As detailed in Cavalheiro et al. (2021), the lower portion of the studied section documents the positive CIE that identifies the Valanginian Weissert Event that is comprised between the top of calcareous nannofossil subzone NC3a and the top of subzone NC3b of Bralower et al. (1995) and Zone BC4 of Bown et al. (1998) (see the chronostratigraphic revision in Cavalheiro et al., 2021) (Fig. 2). Following the original definition by Erba et al. (2004), the onset of the Weissert Event is placed at the base of the positive CIE (sample 113-692B-12R-2, 71-73 cm; 90.57 mbsf; A in Fig. 2) and the end of the event coincides with the top of the CIE plateau (sample 113-692B-10R-4, 61-65 cm; 83.63 mbsf; C in Fig. 2) (Cavalheiro et al., 2021). Carbon isotope values are relatively stable in the Hauterivian - lowermost Barremian interval in core 9R, documenting average values of ~ -30 ‰. Notably, relevant fluctuations of about 2‰ are documented in the topmost intervals in cores 8R (early Barremian in age) and 7R (no age assignment).

The total organic carbon (TOC) values in ODP Hole 692B range from 1.3 to 18%, with an average of 8.0% (Fig. 2). The highest TOC values, up to 14.9-18% (samples 113-692B-9R-1, 92-95 cm and 113-692B-9R-1, 132-135 cm, respectively), are observed in the middle part of the section (Hauterivian - lower Barremian). The lowest TOC content (e.g., 1.3% in sample 113-692B-7R-1, 101-103 cm) is recorded in the topmost stratigraphic interval (core 7).

3.3. Benthic foraminifera

Twenty-two out of 69 samples are barren of BF and, therefore, quantitative analyses were performed on 47 samples that contained scarce (especially in cores 113-692B-7R, 113-692B-8R, and 113-692B-9R) to abundant BF assemblages (Fig. 2, 3), which are composed only of calcareous benthic foraminifera (Figs. 2, 3, 4).

The preservation of BF is good throughout the studied section (Fig. 4). Nevertheless, some tests show moderate etching, suggesting dissolution or slight overgrowth and breakages (especially in samples 113-692B-9R-2, 45-48 cm, 113-692B-9R-1, 60-63 cm, 113-692B-9R-2, 10-13 cm, and 113-692B-10R-6, 39-42 cm). A possible explanation for the diagenetic alteration in terms of dissolution is related to early post-depositional changes in pore water chemistry, which provoke an imbalance with the foraminiferal tests (Murray and Alve, 1999; Kozdon et al., 2013).

The BFN vary between 1 and 481 specimens/10g of dry sediment (Fig. 2). The highest BFN (481 specimens /10g sed) is found in the upper Valanginian (sample 113-692B-10R-6, 82-85 cm) coinciding with the middle part of the Weissert Event, while the lowest BFN value (1 n/10g sed) is recorded at 60.73 mbsf (sample 113-692B-8R-1, 143-146 cm; Fig. 2). The S reaches a high value of 16 taxa in the upper Valanginian (samples 113-692B-10R-5, 125- 128 cm and 113-692B-10R-6, 13- 16 cm) and the middle part of the Weissert Event (Fig. 2). The D values are highest (=1) in the Barremian (samples 113-692B-8R-1, 87-90 cm, 692B-8R-1, 143-146 cm and 113-692B-8R-2, 80- 83 cm; Fig. 2), in which the H_S recorded the lowest values (0). The lowest value of D (=0.13) is detected in the upper Berriasian/lower Valanginian (sample 113-692B-12R-3, 112-115 cm). The highest value of H_S (2.14) was recorded in the upper Valanginian (sample 113-692B-10R-5, 125-128 cm; Fig. 2).

Thirty-three BF taxa (12 genera and 28 species; Supplementary Table S2) were identified in the upper Berriasian to lower Barremian stratigraphic interval in ODP Hole 692B (Fig. 3). The most abundant taxa are represented by the genus *Eoguttulina* (*Eoguttulina bilocularis*, *Eoguttulina biserialis*, *Eoguttulina fusus, Eoguttulina guttifera*), ranging from 1 specimen/10g (in samples at 92.32 mbsf, 79.48 mbsf, 61.19 mbsf, and 60.81 mbsf) to 205 specimens/10g (at 83.55 mbsf). *Eoguttulina bilocularis* is the most abundant species in the BF assemblages, fluctuating from 0.39% (at 85.75 mbsf) to 90.00% (at 90.55 mbsf) (Fig. 3).

The absolute abundance of *Lenticulina* (*Lenticulina* sp. 1., *Lenticulina involvens*, *Lenticulina*

lideri, *Lenticulina pulchella*, *Lenticulina turgidula*) ranges from 1 specimen/10g (samples at 91.49 mbsf, 85.40 mbsf, and 70.75 mbsf) to 319 specimens/10g (at 86.82 mbsf; Fig. 3). The most abundant species is *L. turgidula*, which varies from 0.48% (at 70.75 mbsf) to 33.33% (91.02 mbsf; Fig. 3).

Genus *Laevidentalina* (*Laevidentalina* sp., *Laevidentalina* sp. 1., *Laevidentalina* sp. 2., *Laevidentalina debilis*, *Laevidentalina distincta*, *Laevidentalina guttifera*, *Laevidentalina soluta*), displays low absolute abundance, varying from 1 specimen/10g (samples at 90.55 mbsf, 61.19 mbsf, and 70.75 mbsf) to 53 specimens/10g (at 83.55 mbsf; Fig. 3). *Laevidentalina distincta* is the most abundant species, ranging from 0.52% (at 86.82 mbsf) to 100% (at 60.17 mbsf; Fig. 3).

Genus *Saracenaria* (*Saracenaria* sp., *Saracenaria bronni*, *Saracenaria tsaramandrosoensis*) is characterized by low absolute values varying from 1 specimen/10g (at samples of 92.32 mbsf, 79.48 m, 72.73 mbsf, 72.22 mbsf, 71.45 mbsf, 70.75 mbsf, and 68.95 mbsf) to 69 specimens/10g (at 83.55 mbsf; Fig. 3). *Saracenaria* sp. displays high abundance, fluctuating from 0.48% (70.75 mbsf) to 80% (at 85.40 mbsf) (Fig. 3).

The absolute abundance of *Vaginulinopsis* (*Vaginulinopsis* sp., *Vaginulinopsis enodis*, *Vaginulinopsis excentrica*) is characterized by intermediate values, ranging from 1 specimen/10g (samples at 91.02 mbsf, 70.75 mbsf, and 61.19 mbsf) to 82 specimens/10g (at 85.75) (Fig. 3). The species most abundant is *V. excentrica*, which fluctuates between 15.74% (at 86.82) and 33.33% (at 86.39 mbsf) (Fig. 3).

The previously described assemblages represent about 95% of the total BF and are recorded mainly in the Valanginian- Hauterivian interval (cores 113-692B-9R and 113-692B-10R; Fig. 3). The remaining 5% of the BF assemblages show low abundances and are characterized by *Citharina* sp., which ranges from 1 specimen/10g to 3 specimens/10g (Fig. 3). The abundance of the genus *Lagena* (*Lagena* sp., *Lagena sulcata*, and *Lagena ovata*) ranges from 1 specimen/10g to 26 specimens/10g (Fig. 3). Genus *Marginulina* (*Marginulina* sp., *Marginulina bullata*, *Marginulina gatesi*) fluctuates from 1 specimen/10g

312 to 27 specimens/10g (at 85.75 mbsf) (Fig. 3). *Nodosaria sceptrum* shows a lower value of abundance,
313 between 1 specimen/10g and 2 specimens/10g (Fig.3). The abundance of *Planularia complanata*
314 fluctuates from 1 specimen/10g to 21 specimens/10g (at 85.75 mbsf) (Fig. 3). *Spirilina minima* is
315 recorded in the upper Valanginian with abundances of up to 5 specimens/10g in a sample at 86.13 mbsf
316 and 6 specimens/10g in a sample at 85.75 mbsf (Fig. 3).

317 Benthic foraminifera assemblages display high dominance of the taxa belonging to the infaunal
318 morphogroup (mean value of 98.3%) throughout the studied succession (Fig. 2). The dominant
319 morphogroup is represented by the genera *Citharina*, *Eoguttulina*, *Laevidentalina*, *Lagena*, *Lenticulina*,
320 *Marginulina*, *N*odosaria, *Planularia*, *Saracenaria*, and *Vaginulinopsis* (Fig.3). The remaining 1.7% of
321 the assemblages correspond to the occurrence of *Spirillina minima*, which is considered an epifaunal
322 species that is only registered in the middle part of the Weissert Event (samples 113-692B-10R-5, 125-
323 128 cm and 113-692B-10R-6, 13-16 cm) (Fig. 3).

324

325 **4. Discussion**

326 **4.1 Paleobathymetric evolution**

327 The current configuration of the Antarctic continental margin of the eastern Weddell Sea off Kapp
328 Norvegia (Fig. 5A) shows a very steep and narrow upper continental slope that abruptly passes into a
329 gently sloping mid-slope bench. The transition between the continental rise and the abyssal plain (> 4000
330 m water depth) is characterized by the steep and narrow Explora Escarpment (Hinz and Krause, 1982;
331 Barker et al., 1988).

332 The ODP Hole 692B was drilled at 2875 m water depth, and the oldest sedimentary rocks were
333 recovered at 97.9 mbsf, approximately in the mid-slope bench of the Wegner Canyon (upper scarp),
334 corresponding to the abyssal zone (Fig. 5A).

335 The most abundant genus is *Eoguttulina*, which has been described as inhabiting in shelf

environments (e.g., Georges Bank basin - USA; Scholle and Wenkam 1982) and outer neritic to upper bathyal settings (e.g., Sergipe - Brazil; Koutsoukos, 1989). *Eoguttulina bilocularis*, the most abundant species in the studied interval at Hole 692B, was documented by Riegraf (1989) on a shallow shelf in the Indian Ocean (DSDP Site 249). *Laevidentalina*, *Lenticulina, Lagena*, and *Nodosaria* have a broad paleobathymetric range, occurring from inner neritic to lower bathyal environments (Table 1). *Saracenaria* was allocated to an inner-to outer neritic setting by Frenzel (2000) and a neritic to a middle bathyal environment by Koutsoukos (1989). *Vaginulinopsis* is reported as bathyal in the Indian Ocean (e.g., Holbourn and Kaminski, 1995a). Based on the known paleobathymetric distribution of the taxa detected in this study (Table 1) and thanks to the high-resolution sampling adopted, an outer neritic-upper bathyal (~200 - 500 m) bathymetric deposition is inferred for ODP Hole 692B at the upper Berriasian - Barremian interval (Fig. 5B), contrasting with the earlier estimation (500 - 1000 m) given by Barker et al. (1988).

According to Barker et al. (1988), the BF taxa recorded in the Pliocene and Pleistocene sediments in ODP Hole 692B indicate a bathymetry not significantly different from the present water depth (2875 m). Furthermore, at the nearby ODP Site 693, benthic foraminifera also indicate an outer neritic-upper bathyal setting (200 - 500 m) during the Aptian - Albian, and a paleodepth similar to the present water depth (about 2400 m) is inferred for the Miocene - Pleistocene time interval (Barker et al., 1988; Leckie, 1990). Therefore, according to these data, the evolution of the Weddell Sea displays a progressive deepening of the basin, passing from an outer neritic-upper bathyal setting during the Early Cretaceous (Berriasian-Barremian in ODP Hole 692B, Aptian - Albian at ODP Site 693) to ultra-deep waters (abyssal) at present.

4.2 Paleoecological significance of benthic foraminifera

Despite the lack of a continuous sedimentary record and the low abundance of benthic foraminifera

(BFN; Fig. 2) throughout the ODP Hole 692B, the BFN, the diversity indices (D-H_S; Fig. 2), paleoecological preferences of the identified taxa, and statistical analyses (NMDS and DCA; Figs. 6A, 6B), allowed a detailed palaeoenvironmental reconstruction of the bottom-water conditions during the Lower Cretaceous.

The BFN and diversity indices (D - H_S) are well established in the literature and used to estimate the oxygen content and the organic-matter flux to bottom waters (e.g., Sen Gupta and Machain-Castillo, 1993; Kaiho and Hasegawa, 1994; Jorissen et al., 1995; van der Zwaan et al., 1999; Friedrich et al., 2006; Jorissen et al., 2007). The BFN changes recorded in ODP Hole 692B probably reflect fluctuations in organic matter flux associated with dissolved oxygen availability. The increase in BFN recorded in the upper Valanginian (samples 113-692B-10R-6, 82-85 cm, 113-692B-10R-6, 13-16 cm, 113-692B-10R-5, 125-128 cm, 113-692B-10R-4, 55-58 cm, 113-692B-10R-4, 22-25 cm, 113-692B-10R-3, 115-118 cm, and 113-692B-9R-2, 115-117.5 cm) and upper Hauterivian (sample 113-692B-9R-2, 45-48 cm) could represent the response to enhanced organic-matter flux and/or decreased oxygen availability in bottom waters (e.g., Gooday, 2003; Schmiedl et al., 1998; Holbourn et al., 2001b; Friedrich et al., 2006; Friedrich and Hemleben, 2007). Diversity (H_S) in ODP Hole 692B is characterized by low to intermediate values, fluctuating between 0 and 2.1, indicating stressing conditions under low oxygen and high organic-matter fluxes to the seafloor. In turn, the high values of D in the upper Valanginian (samples 113-692B-12R-2, 85-88 cm, 113-692B-12R-2, 29-32 cm, 113-692B-10R-5, 90-93 cm, and 113-692B-10R-3, 11-14 cm), lower Hauterivian (sample 113-692B-10R-1, 67-70 cm), upper Hauterivian (sample 113-692B-9R-2, 45-48 cm), and Barremian (samples 113-692B-8R-2, 26-29 cm, 113-692B-8R-2, 80-83 cm, 113-692B-8R-2, 1-4 cm, 113-692B-8R-1, 143-146 cm, 113-692B-8R-1, 87-90 cm, and 113-692B-7R-2, 138-141 cm) suggest a decline in oxygen but high nutrient availability in bottom waters (Fig. 2). Similar bottom water conditions have been described in various locations worldwide during the Cretaceous (e.g., Holbourn et al., 2001b; Friedrich et al., 2005a; Friedrich et al., 2006).

The significance of BF assemblages in reconstructing the link between organic carbon flux (food availability) and oxygenation of the bottom waters has been shown by several authors (e.g., Bernhard, 1986; Jorissen et al., 1995; van der Zwaan et al., 1999; Jorissen, 1999; Jorissen et al., 2007). The Lower Cretaceous BF assemblages in ODP Hole 692B display an absolute predominance of infaunal taxa (Fig. 2), which are characterized by their dependence on the intermittent flux of labile and easily metabolized organic matter to the seafloor and oxygen-depleted environments (e.g., Corliss and Chen, 1988; Sen Gupta and Machain-Castillo, 1993; Kaiho, 1994; Kaminski et al., 1995; Jorissen et al., 1995; Erbacher et al., 1998; Jorissen, 1999; Holbourn et al., 2001b; Friedrich et al., 2003; 2006; see Table 1).

Eoguttulina, the most abundant genus within the assemblage in Hole 692B (Fig. 3), is interpreted to be an opportunist taxon at different locations, characterized by preferring environments with reduced levels of oxygen and high organic matter at the sediment-water interface during Jurassic times (e.g., Dorset Coast-England: Hart and Fitzpatrick, 1995; Middle Atlas-Morocco: Reolid et al., 2013; Lusitanian Basin-Portugal: Reolid et al., 2019; Cueva del Agua-Spain: Reolid, 2020). Moreover, *Eoguttulina* was recorded in the oxygen-depleted sediments of the Cretaceous Sergipe Basin in Brazil (e.g., Koutsoukos, 1989). The genus *Laevidentalina* is known as a dysoxic indicator, able to live under depleted oxygen conditions (Kahio and Hasegawa, 1994; Frenzel, 2000) and is interpreted from Cretaceous black-shale intervals as highly tolerant to low oxygen levels and high organic carbon fluxes (Friedrich and Erbacher, 2006; Koch and Friedrich, 2012). Genus *Saracenaria* was found in dysaerobic to quasi-anaerobic environments of the upper Aptian-lower Albian in the Sergipe Basin (Koutsoukos, 1989; Koutsoukos and Hart, 1990) and is considered to thrive under suboxic conditions (Alegret et al., 2003).

The genus *Lenticulina* is an opportunist taxon thriving under low oxygen concentrations and high organic-matter fluxes; it has been documented worldwide in different basins during the Jurassic and Cretaceous (Koutsoukos and Hart, 1990; Tyszka, 1994; Kahio, 1994; Frenzel, 2000; Holbourn et al., 2001b; Reolid et al., 2013; Aschckenazi-Polivoda et al., 2018; Giraldo-Gómez et al., 2018).

Vaginulinopsis excentrica was recorded in dark claystones at DSDP Site 263 in the Indian Ocean during the Valanginian-Barremian time interval and interpreted as an indicator of high organic-matter influx coupled with oxygen-depletion (Holbourn and Kaminski, 1995b). *Vaginulinopsis enodis* was found in restricted bottom waters associated with a considerable supply of organic matter during the Jurassic (e.g., Svalbard: Løfaldli and Nagy, 1980). The genus *Marginulina* was recorded in oxygen-depleted bottom waters characterized by an ample supply of organic matter during the Jurassic (Løfaldli and Nagy, 1980) and was also observed in dysaerobic conditions with changing oxygen concentration at the seafloor during the Hauterivian in Austria (Eastern Alps: Decker and Rögl, 1998).

High organic-matter fluxes are also evidenced by the occurrence of diagnostic taxa in ODP Hole 692B such as *Eoguttulina* (e.g., Koutsoukos, 1989; Hart and Fitzpatrick, 1995; Reolid et al., 2013; Reolid et al., 2019; Reolid, 2020), *Lenticulina* (e.g., Koutsoukos and Hart, 1990; Tyszka, 1994; Kahio, 1994; Frenzel, 2000; Holbourn et al., 2001b; Reolid et al., 2013; Aschckenazi-Polivoda et al., 2018; Giraldo-Gómez et al., 2018), *Laevidentalina* (e.g., Friedrich and Erbacher, 2006; Koch and Friedrich, 2012), *Marginulina* (e.g., Løfaldli and Nagy, 1980; Decker and Rögl, 1998), and *Vaginulinopsis* (e.g., Svalbard: Løfaldli and Nagy, 1980; Holbourn and Kaminski, 1995b) are more abundant under eutrophic conditions (higher organic-matter fluxes), where they can reach high relative abundance (> 90%) (Fig. 7). In summary, the assemblages recorded in ODP Hole 692B display typical taxa that thrived under depleted oxygen conditions with an enhanced increase of organic carbon flux under eutrophic conditions, where bottom water oxygenation become the dominant control on the composition of foraminiferal assemblages (e.g., Jorissen et al., 1995; van Der Zwaan et al., 1999).

Non-metric multidimensional scaling (NMDS) ordination displays an arrangement of the Lower Cretaceous BF in ODP Hole 692B that shows different relationships with various proxies such as TOC, BFN, D, and H_S in two dimensions (Fig. 6A). The correlation between BFN and H_S with TOC values shows different combinations according to the NMDS, as follows (Fig. 6A): a) highest TOC with very

few or no BFN and very low Hs; b) moderate to elevate TOC with high BFN and Hs values; c) low TOC with high BFN and Hs values. High TOC content is interpreted to reflect increased organic-matter fluxes (food) that might result from enhanced preservation, deriving from an additional supply of terrestrial organic matter or increased surface water productivity (Wahyudi and Minagawa, 1997; Gooday et al., 2009; Lowery et al., 2014).

A Detrended Correspondence Analysis (DCA) was carried out to evaluate the principal environmental gradients controlling the distribution of benthic foraminifera. The first axis of the DCA (Fig. 6B) mainly separates two BF patterns. The right side of the DCA displays positive scores and is characterized by *Citharina*, *Eoguttulina*, *Laevidentalina*, *Lagena*, *Marginulina*, *N. sceptrum*, *P. complanata*, *Saracenaria*, *S. minima* and *Vaginulinopsis*, while on the left side is only observed *Lenticulina* with negative scores. Based on the ecological preferences described above, the first axis likely represents changes in productivity (carbon-organic flux) in bottom-waters. In addition, the low negative scores of *Eoguttulina* and *Lenticulina* are opposite to the remaining taxa (*Citharina*, *Laevidentalina*, *Lagena*, *Marginulina*, *N. sceptrum*, *P. complanata*, *Saracenaria*, *S. minima* and *Vaginulinopsis*) that display positive scores. According to this distribution, the second axis of the DCA (Fig. 6b) probably reflects oxygen-depletion conditions (moderate to extremely dysoxic conditions) in bottom waters.

However, the potential changes in the bottom waters, evidenced by different proxies, allow concluding that the short-term fluctuations in the BFN and an increase in Hs in ODP Hole 692B reflect the presence of oxygen in the seabed during short intervals in the upper Valanginian (samples 113-692B -10R-6, 82-85 cm, 113-692B-10R-5, 125-128 cm, 113-692B-10R-4, 55-58 cm, 113-692B -10R-4, 22-25 cm, and 113-692B-10R-3, 115-118 cm) and upper Hauterivian (sample 113-692B-9R-2, 45-48 cm). These temporary oxygenation episodes coincide with a slight increase in abundance of the genus *Lenticulina* and a decrease in TOC values, especially in the upper Valanginian (Figs. 2, 3). In turn, an

opposite correlation between *Lenticulina* and *Eoguttulina* is evidenced by the DCA, indicating that *Lenticulina* is more controlled by the availability of oxygen than *Eoguttulina*; the latter taxon is more dependent on food (organic carbon flux), and both thrived under low oxygen conditions (Fig. 6B).

4.3 The Weissert Event in the Weddell Sea

The late Valanginian Weissert Event corresponds to a large-scale perturbation in the global carbon cycle, affecting both the atmosphere and ocean systems, as evidenced by a positive carbon isotope excursion (CIE) in marine and terrestrial settings (e.g., Erba et al., 2004; Meissner et al., 2015). In ODP Hole 692B, a well-defined $\delta^{13}C$ carbon isotopic excursion is documented by Cavalheiro et al. (2021) (Figs. 2, 7).

The new data gathered in this study of the benthic foraminiferal assemblages across the Weissert Event reveals variations in abundances (BFN), diversity indices (D and Hs) and composition, allowing identification of intervals characterized by specific environmental conditions coinciding with decreases and increases in organic carbon fluxes and oxygen content in bottom waters (Fig. 7).

Before the perturbation (pre-Weissert Event), the bottom-waters experienced dysoxic conditions with high organic-matter fluxes (interval 1; Fig. 7). At the onset of the Weissert Event (A in Figs. 2, 7), a progressive deterioration of the bottom waters under extremely dysoxic conditions and high organic carbon flux were recorded (interval 2; Fig. 7). The absence of BF suggests a transition to anoxic conditions recorded in the bottom waters, which coincides with the first peak of the Weissert CIE (B in Figs. 2, 7). Between the first peak of the Weissert perturbation (peak B in Fig. 7) and the end of the carbon isotopic plateau (peak C in Figs. 2, 7), and above the interval barren of BF, the assemblages suggest a sporadic increase in oxygen concentration (moderate dysoxic conditions), which favored the recolonization of bottom waters (interval 4; Fig. 7). Similar repopulation events have been described for other Oceanic Anoxic Events (e.g., Friedrich, 2010; Friedrich et al., 2005b, 2011), indicating short-term

amelioration of bottom waters during overall hostile conditions. The latest part of the Weissert CIE near the end of the carbon isotopic plateau displays a sudden decrease in the oxygen concentration of the seafloor, with severe dysoxia, marked by an abrupt reduction in the BFN (interval 5; Fig. 7).

In the recovery state of the Weissert CIE (post-peak C in Fig. 7), it is evident that the BFN rapidly increases, indicating a reinvigorated repopulation phase whose magnitude is similar to the previous one detected after the interval of most severe anoxia. An improvement in the seafloor as evidenced by an increase in oxygen concentration is compared with the preceding interval marked by several dysoxic conditions under high organic carbon flux (interval 6; Fig. 7). Moreover, this increase in BF abundance and species richness correlates with a cooling episode documented by micropaleontological, mineralogical, and geochemical proxies (Erba et al., 2004; Cavalheiro et al., 2021; Fig. 7) and, thus, might have been triggered by the downwelling of colder and denser surface waters, resulting in oxygen-rich bottom waters that favored benthic organisms. The Valanginian - Hauterivian boundary was characterized by a significant decrease in the BFN, indicating oxygen-depleted bottom waters characterized by severe dysoxic conditions under moderate organic-carbon flux (interval 7; Fig. 7).

4.4 Paleoceanography of the Weddell Sea during the Early Cretaceous

The paleoceanography in the Antarctic region during the Early Cretaceous was closely related to the stretching and eventual separation of the West Antarctic Peninsula from East Antarctica, which originated the Weddell Sea in response to the early evolution of the South Atlantic and the western Indian Ocean (Owen, 1983; Crame, 1999).

According to the data described in this study, the Lower Cretaceous sedimentary sequence recovered in ODP Hole 692B was deposited at a paleo-water depth of 200 - 500 m in an outer neritic-upper bathyal setting, characterized by high TOC contents (Fig. 2) and abundant pyrite framboids (Fig. 7), which are generally used to reconstruct paleo-redox conditions. These high-TOC values resulted from

the enhanced burial of organic- carbon deposited under anoxic and euxinic bottom water conditions. The distribution of pyrite framboids allows determining their character syngenetic (formed in the water column) or diagenetic (originated within the sediment), suggesting anoxic-euxinic or dysoxic conditions, respectively (Wignall and Newton, 1998; Bond and Wignall, 2010; Dummann et al., 2021).

The frequent abundance of radiolarians throughout the investigated interval may indicate enhanced nutrient levels in the surface waters (Fig. 7). Similarly, the occurrence of abundant calcispheres, possibly colonizing the niches left vacant by the collapse of the dinoflagellate cyst population (e.g., Hart, 1991), supports stressing conditions in the surface waters (Fig. 7).

A relevant cooling episode coinciding with the end of the Weissert Event is documented in ODP 692B in the Weddell Sea, displaying a ~3-4 °C decline in the sea surface temperature (SST) derived from TEX_{86} analyses (Cavalheiro et al., 2021; Fig. 7). This cooling is consistent with global signals based on different SST-proxies that document more pronounced temperatures sensitive to the climate in high-latitude regions (Cavalheiro et al., 2021). The presence of abundant benthic foraminifera during the Weisser Event (interval 4; Fig 7) coincides with a cooling episode, indicating a significant increase in oxygen in bottom waters after a period of anoxic conditions (interval 3; Fig 7). A benthic foraminiferal repopulation event is generally linked to increased oxygen concentrations for a short time. Similar repopulation events have been reported in different OAEs (OAE 1b: Friedrich et al., 2005b; OAE 2: Friedrich et al., 2011) and from Quaternary Mediterranean sapropels (e.g., Rohling et al., 1997; Schmiedl et al., 2003; Friedrich et al., 2005b). Different mechanisms have been postulated to explain these repopulation events, which could be triggered either by a decrease in nutrient input from the surface waters or/and by an increase in the ventilation of bottom waters during cooling periods characterized by short-term climate variability (Rohling et al., 2002; Friedrich et al., 2005b, 2011). Based on benthic foraminiferal assemblages recorded in ODP Hole 692B, we hypothesize that the repopulation event in the Weddell Sea could be related to short periods of oxygenation-ventilation rather than to a decrease in

528 the supply of nutrients in the bottom waters (interval 4; Fig. 7).

529 In the lower Hauterivian, a continuous decline in oxygen availability induced severely dysoxic to
530 anoxic conditions with increased organic-carbon fluxes (interval 8; Fig. 7). In the uppermost lower
531 Hauterivian, the bottom waters display a depleted-oxygen availability under dysoxic to anoxic conditions
532 characterized by several increases in organic carbon fluxes. Subsequently, it is evidenced a sudden
533 increase in oxygen availability and moderate dysoxic conditions, as well as with by high organic carbon
534 flux in the seafloor (intervals 9 and 10; Fig. 7). The previously mentioned bottom-water conditions
535 remained during the upper Hauterivian (interval 10; Fig. 7).

536 The lower Barremian and the post-Barremian stratigraphic interval indicates a transition to a more
537 stressful environmental setting, suggesting extremely dysoxic to anoxic bottom conditions, with high
538 organic carbon flux (intervals 11 and 12; Fig. 7), whereas the topmost studied sequence, characterized
539 by the absence of benthic foraminifera, indicates anoxic-water conditions (interval 13; Fig. 7).

540 Micropaleontological, geochemical and sedimentological data from ODP Hole 692B indicate
541 paleoceanographic changes that influenced the Weddell Sea during the Lower Cretaceous. A dominance
542 of anoxic-euxinic and dysoxic conditions is further supported by the scarcity of benthic foraminiferal
543 assemblages and by the presence of organic-rich sediments with high TOC content and pyrite framboids.

544 Food availability is strongly related to organic-carbon fluxes and the transport of organic matter to
545 the seafloor. Therefore, a relationship between benthic foraminiferal assemblage and depositional
546 environments is observed. Marine coastal settings are generally characterized by organic-rich sediments
547 resulting from enriched supplies of terrestrial organic matter and enhanced productivity via runoff.
548 However, the lack of terrestrial siliciclastic and organic material in ODP Hole 692B (O'Connell, 1990;
549 Robert and Maillot, 1990) discards a relationship between high TOC content and primary productivity
550 associated with a runoff system.

551 We hypothesize that the enhanced organic matter availability in bottom waters (as a food supply),

552 as evidenced by the infaunal assemblages of benthic foraminifera in the Weddell Sea, probably reflected
553 a local upwelling system favored by climatic and atmospheric circulation (O'Connell, 1990). The
554 evidence of radiolarians in ODP Hole 692B may support the idea of an upwelling system as suggested
555 by comparison with the modern radiolarian blooms, which characterize high-fertility upwelling regions
556 where increased nutrient loadings (phosphates and nitrates) are combined with enhanced silica
557 availability (Racki and Cordey, 2000). Recent studies on modern upwelling systems indicate variability
558 of climate factors such as changes in local wind forcing, ventilation processes, or the source-water
559 pathways, which influence oxygen concentration availability, nutrient supply, and CO_2 concentrations in
560 the surface waters (Rykaczewski and Dunne, 2010; García-Reyes et al., 2015).

561 The proto-Drake Passage between South America and the Antarctic Peninsula has been described
562 as a narrow and shallow connection during the Barremian to Albian (Sewall et al., 2007; Eagles, 2016).
563 However, new circulation models in the proto-Drake Passage suggest that from the Berriasian to
564 Hauterivian, there was a sluggish water mass exchange between the Southern Ocean and the South
565 Pacific with the adjacent proto-Indian and Tethys Oceans (Dummann et al., 2021). On the contrary, a
566 West-to-East transport of intermediate water masses between the Pacific and the Southern Ocean is
567 proposed to have occurred since the Barremian (Dummann et al., 2021).

568 We may therefore postulate that possible bottom currents owing to the influx of Southern Ocean
569 waters favored short-term pulses of ventilation in the Weddell Sea under constant increased organic-
570 carbon flux during the upper Valanginian and upper Hauterivian (intervals 4, 6, and 10; Fig 7).

571 The documented BF assemblages occurring in the Weddell Sea show similarities to those observed
572 in the Boreal and Tethyan bioprovinces and reveal a strong affinity with the Austral bioprovince of the
573 southern hemisphere (Sheibnerová, 1973; 1976). In particular, Lower Cretaceous BF recorded in ODP
574 Hole 692B display an affinity with assemblages from South-America (e.g., the Austral Basin of southern
575 Patagonia and the Andean Basin: Riccardi, 1988; Bertels, 1988), the Indian Ocean (e.g., Mozambique

ridge - DSDP Site 249: Riegraf, 1989, Holbourn and Kaminski, 1994), and Australia (e.g., Great Australian Basin: Sheibnerová, 1976; Exmouth Plateau off northwest Australia ODP Site 766: Holbourn and Kaminski, 1994; Holbourn and Kaminski, 1995a).

Such affinities of benthic foraminifera argue for an efficient exchange of circulation across the Southern Ocean sub-basins, with cosmopolitan BF populating the Austral realm (e.g., Sheibnerová, 1973; 1976), excluding restricted conditions at the Weddell Sea during the Lower Cretaceous.

5. Conclusions

Detailed benthic foraminiferal data from the Weddell Sea (ODP Hole 692B, Antarctica) suggests variable bottom water conditions in the latest Berriasian to Barremian time interval in terms of organic-carbon fluxes and oxygenation at the seafloor.

1. A paleodepth corresponding to an outer neritic-upper bathyal setting (~200 - 500 m) is inferred by benthic foraminiferal assemblages through the late Berriasian to early Barremian time interval.
2. Benthic foraminiferal assemblages show significant variation in the BFN and diversity indices (D and H_S), indicating changes in bottom waters. Low abundances and diversities of benthic foraminiferal assemblages suggest prevailing high organic matter-fluxes and strongly dysoxic- to anoxic conditions at the seafloor in the Weddell Sea. Brief interruptions with a slight increase in bottom-water oxygenation occurred during and after the Weissert Event, in the latest Valanginian and late Hauterivian.
3. Benthic foraminiferal assemblages are dominated by infaunal taxa (*Eoguttulina*, *Laevidentalina*, *Lagena*, *Lenticulina*, *Marginulina*, *N*odosaria, *Planularia*, *Saracenaria*, and *Vaginulinopsis*) tolerant to depleted-oxygen conditions and high organic-matter fluxes.
4. Food supply, identified by high organic-matter flux, was not the main factor controlling benthic

foraminiferal assemblages. Instead, the redox state of bottom waters seems to have had overall control in the Weddell Sea.

5. During the Weissert Event, stressful bottom water conditions include short-term severely dysoxic conditions (Weissert CIE onset), culminating in an anoxic interval characterized by the absence of benthic foraminifera (peak B of the Weissert Event). Re-oxygenation interludes favored the return of benthic foraminifera, known as a repopulation event, which coincided with a global cooling episode at the end of the Weissert Event (between peaks B and C).
6. Brief pulses of increases in oxygen concentrations in the bottom waters during and after the Weissert Event (late Valanginian) and late Hauterivian were probably originated by bottom currents, which promoted the ventilation under a constant increase in organic carbon flux.

Acknowledgments

We thank the Ocean Drilling Program (ODP) for providing samples used in this study. Eni Spa is acknowledged for financial support and permission to publish this study. This research was funded through PRIN 2017RX9XXY to E. Erba. The authors also acknowledge the support of the Italian Ministry of University (MUR) through the project "Dipartimenti di Eccellenza 2018-2022, Le Geoscienze per la Società: Risorse e loro evoluzione". We thank the editor and anonymous reviewers for their helpful comments and suggestions. Thanks to Stefania Crespi for her assistance at the Scanning Electron Microscope.

References

Aguado, R., Company, M., Castro, J. M., de Gea, G. A., Molina, J. M., Nieto, L. M., Ruiz-Ortiz, P. A., 2018. A new record of the Weissert episode from the Valanginian succession of Cehegín (Subbetic,

SE Spain): Bio-and carbon isotope stratigraphy. Cretaceous Res. 92, 122-137.

Alegret, L., Molina, E., Thomas, E., 2003. Benthic foraminiferal turnover across the Cretaceous/Paleogene boundary at Agost (southeastern Spain): paleoenvironmental inferences. Mar. Micropaleontol. 48 (3-4), 251-279.

Applegate, J. L., Bergen, J. A., 1988. Cretaceous calcareous nannofossil biostratigraphy of sediments recovered from the Galicia Margin, ODP Leg 103. Proc Ocean Drill Prog Sci Results. 103, 293-348.

Arthur, M. A., Schlanger, S. O., 1979. Cretaceous "Oceanic Anoxic Events" as causal factors in development of reef-reservoired giant oil fields. AAPG Bull. 63, 870-885.

Arthur, M. A., Brumsack, H. J., Jenkyns, H. C., Schlanger, S. O., 1990. Stratigraphy, geochemistry, and paleoceanography of organic carbon-rich Cretaceous sequences. In Cretaceous resources, events and rhythms. Springer, Dordrecht. pp. 75-119.

Arthur, M. A., Sageman, B. B., 1994. Marine black shales: depositional mechanisms and environments of ancient deposits. Annu. Rev. Earth Planet. Sci. 22(1), 499-551.

Ashckenazi-Polivoda, S., Titelboim, D., Meilijson, A., Almogi-Labin, A., Abramovich, S., 2018. Bathymetric trend of Late Cretaceous southern Tethys upwelling regime based on benthic foraminifera. Cretaceous Res. 82, 40-55.

Barbarin, N., Bonin, A., Mattioli, E., Pucéat, E., Cappetta, H., Gréselle, B., Joachimski, M., 2012.

Evidence for a complex Valanginian nannoconid decline in the Vocontian basin (South East France). Mar. Micropaleontol. 84, 37-53.

Barker, P. F., Kennett, J. P., 1988. Sites 691 and 692. Init. Rep. Deep Sea Drill. Proj. 113, 293-328.

Bernhard, J. M., 1986. Characteristic assemblages and morphologies of benthic foraminifera from anoxic, organic-rich deposits; Jurassic through Holocene. J. Foraminiferal Res. 16(3), 207-215.

Bertels, A., 1988. Cretaceous foraminifera of Argentina: biogeographic tendences. Rev. Bras. Geociênc. 18(3), 299-311.

Bond, D. P., Wignall, P. B., 2010. Pyrite framboid study of marine Permian-Triassic boundary sections: a complex anoxic event and its relationship to contemporaneous mass extinction. Geol. Soc. Am. Bull. 122, 1265-1279.

Bottini, C., Erba, E., 2018. Mid-Cretaceous paleoenvironmental changes in the western Tethys. Clim. Past. 14(8), 1147-1163.

Bornemann, A., Mutterlose, J., 2008. Calcareous Nannofossil and $\delta^{13}C$ records from the Early Cretaceous of the Western Atlantic Ocean: Evidence for enhanced fertilization across the Berriasian-Valanginian transition. Palaios 23, 821-832.

Bown, P, R., Rutledge, D., Crux, J, A., Gallagher, L, T., 1988. Lower Cretaceous. In Bown, P. (Ed) Calcareous Nannofossil Biostratigraphy. Chapman and Hall, London. pp. 86-131

672 Bralower, T. J., Leckie, R. M., Sliter, W. V., Thierstein, H. R., 1995. An integrated Cretaceous microfossil
673 biostratigraphy. In Geochronology, time scales and global stratigraphic correlation. SEPM Special
674 Publication 54, Society for Sedimentary Geology, Tulsa. 65-79.
675
676 Cavalheiro. L., Wagner, T., Steinig, S., Bottini, C., Dummann, W., Esegbue, O., Gambacorta, G., Giraldo-
677 Gómez, V., Farnsworth, A., Flögel, S., Hofmann, P., Lunt, D., Rethemeyer, J., Torricelli, S., Erba, E.,
678 (Accepted). Impact of global cooling on Early Cretaceous high pCO_2 world during the Weissert Event.
679 Nat. Commun.
680
681 Cetean, C. G., Bălc, R., Kaminski, M. A., Filipescu, S., 2011. Integrated biostratigraphy and
682 palaeoenvironments of an upper Santonian–upper Campanian succession from the southern part of
683 the Eastern Carpathians, Romania. Cretaceous Res. 32 (5), 575-590.
684
685 Channell, J. E. T., Erba, E., Lini, A., 1993. Magnetostratigraphic calibration of the Late Valanginian
686 carbon isotope event in pelagic limestones from Northern Italy and Switzerland. Earth Planet Sci Lett.
687 118(1-4), 145-166.
688
689 Charbonnier, G., Boulila, S., Gardin, S., Duchamp-Alphonse, S., Adatte, T., Spangenberg, J. E., Galbrun,
690 B., 2013. Astronomical calibration of the Valanginian "Weissert" episode: the Orpierre marl–
691 limestone succession (Vocontian Basin, southeastern France). Cretaceous Res. 45, 25-42.
692
693 Corliss, B. H., Chen, C., 1988. Morphotype patterns of Norwegian Sea deep-sea benthic foraminifera
694 and ecological implications. Geology. 16 (8), 716-719.
695

Crame, J. A., 1999. An evolutionary perspective on marine faunal connections between southernmost South America and Antarctica. Sci. Mar. 63, 1-14.

De Azevedo, R. L. M., Gomide, J., Viviers, M. C., 1987. Geo-história da Bacia de Campos, Brasil: do Albiano ao Maastrichtiano. Rev. Bras. Geociênc. 17 (2), 139-146.

Decker, K., Rögl, F., 1988. Early Cretaceous agglutinated foraminifera from limestone-marly rhythmites of the Gresten Klippen Belt (Eastern Alps Austria). Abh. Geol. Bundesanst. 41, 41-59.

Duchamp-Alphonse, S., Gardin, S., Fiet, N., Bartolini, A., Blamart, D., Pagel, M., 2007. Fertilization of the northwestern Tethys (Vocontian basin, SE France) during the Valanginian carbon isotope perturbation: evidence from calcareous nannofossils and trace element data. Palaeogeogr. Palaeoclimatol. Palaeoecol. 243(1-2), 132-151.

Dummann, W., Hofmann, P., Herrle, J. O., Wennrich, V., Wagner, T., 2021. A refined model of Early Cretaceous South Atlantic–Southern Ocean gateway evolution based on high-resolution data from DSDP Site 511 (Falkland Plateau). Palaeogeogr. Palaeoclimatol. Palaeoecol. 562, 1-14.

Eagles, G., 2016. Plate kinematics of the Rocas Verdes Basin and Patagonian orocline. Gondwana Res. 37, 98-109.

Ellis, B. F., Messina, A. R., 1940. Catalogue of foraminifera (Vol. 149). American museum of natural history. http://www.micropress.org.

720 Erba, E., Quadrio, B., 1987. Biostratigrafia a Nannofossili calcarei Calpionellidi e Foraminiferi
721 planctonici della Maiolica (Titoniano superiore—Aptiano) nelle Prealpi Bresciane (Italia
722 settentrionale). Riv. Ital. Paleontol. Stratigr. 93(1), 3-108.
723
724 Erba, E., Bartolini, A., Larson, R. L., 2004. Valanginian Weissert oceanic anoxic event. Geology. 32(2),
725 149-152.
726
727 Erba, E., Bottini, C., Faucher, G., Gambacorta, G., Visentin, S., 2019. The response of calcareous
728 nannoplankton to Oceanic Anoxic Events: The Italian pelagic record. Soc. Paleontol. Ital. 58, 51-71.
729
730 Erbacher, J., Gerth, W., Schmiedl, G., Hemleben, C., 1998. Benthic foraminiferal assemblages of late
731 Aptian-early Albian black shale intervals in the Vocontian Basin, SE France. Cretaceous Res. 19(6),
732 805-826.
733
734 Frenzel, P., 2000. Die benthischen Foraminiferen der Rügener Schreibkreide (Unter-Maastricht, NE-
735 Deutschland). Neues. Palaontol. Abh. 3, 1-361.
736
737 Friedrich, O., 2010. Benthic foraminifera and their role to decipher paleoenvironment during mid-
738 Cretaceous Oceanic Anoxic Events–the “anoxic benthic foraminifera” paradox. Rev. de
739 Micropaleontol. 53(3), 175-192.
740
741 Friedrich, O., Erbacher, J., 2006. Benthic foraminiferal assemblages from Demerara Rise (ODP Leg 207,
742 western tropical Atlantic): possible evidence for a progressive opening of the Equatorial Atlantic
743 Gateway. Cretaceous Res. 27 (3), 377-397.

744

745 Friedrich, O., Hemleben, C., 2007. Early Maastrichtian benthic foraminiferal assemblages from the
746 western North Atlantic (Blake Nose) and their relation to paleoenvironmental changes. Mar.
747 Micropaleontol. 62(1), 31-44.

748

749 Friedrich, O., Reichelt, K., Herrle, J. O., Lehmann, J., Pross, J., Hemleben, C., 2003. Formation of the
750 Late Aptian Niveau Fallot black shales in the Vocontian Basin (SE France): evidence from
751 foraminifera, palynomorphs, and stable isotopes. Mar. Micropaleontol. 49 (1-2), 65-85.

752

753 Friedrich, O., Herrle, J. O., Hemleben, C., 2005a. Climatic changes in the late Campanian-early
754 Maastrichtian: Micropaleontological and stable isotopic evidence from an epicontinental sea. J.
755 Foraminiferal Res. 35 (3), 228-247.

756

757 Friedrich, O., Nishi, H., PROSS, J., Schmiedl, G., Hemleben, C., 2005b. Millennial-to centennial-scale
758 interruptions of the Oceanic Anoxic Event 1b (Early Albian, mid-Cretaceous) inferred from benthic
759 foraminiferal repopulation events. Palaios. 20(1), 64-77.

760

761 Friedrich, O., Erbacher, J., Mutterlose, J., 2006. Paleoenvironmental changes across the
762 Cenomanian/Turonian boundary event (oceanic anoxic event 2) as indicated by benthic foraminifera
763 from the Demerara Rise (ODP Leg 207). Rev. de Micropaleontol. 49 (3), 121-139.

764

765 Friedrich, O., Erbacher, J., Wilson, P. A., Moriya, K., Mutterlose, J., 2009. Paleoenvironmental changes
766 across the Mid Cenomanian Event in the tropical Atlantic Ocean (Demerara Rise, ODP Leg 207)
767 inferred from benthic foraminiferal assemblages. Mar. Micropaleontol. 71(1-2), 28-40.

Friedrich, O., Voigt, S., Kuhnt, T., Koch, M. C., 2011. Repeated bottom-water oxygenation during OAE 2: timing and duration of short-lived benthic foraminiferal repopulation events (Wunstorf, northern Germany). J Micropalaeontol. 30(2), 119-128.

Fütterer, D., Kuhn, G., and Schenke, H. W., 1990. Wegener Canyon bathymetry and results from rock dredging near ODP Sites 691-693, eastern Weddell Sea, Antarctica. Proc Ocean Drill Prog Sci Results. 113, 39-48.

García-Reyes, M., Sydeman, W. J., Schoeman, D. S., Rykaczewski, R. R., Black, B. A., Smit, A. J., Bograd, S. J., 2015. Under pressure: Climate change, upwelling, and eastern boundary upwelling ecosystems. Fron. Mar. Sci. 2(109), 1-10.

Giraldo-Gómez, V. M., Beik, I., Podlaha, O. G., Mutterlose, J., 2018. A paleoenvironmental analyses of benthic foraminifera from Upper Cretaceous–lower Paleocene oil shales of Jordan. Cretaceous Res. 91, 1-13.

Gooday, A. J., 2003. Benthic foraminifera (Protista) as tools in deep-water palaeoceanography: environmental influences on faunal characteristics. In, Southward, A. J., Tyler, P. A., Young, C. M. and Fuiman, L. A. (eds.) Advances in Marine Biology, Vol. 46. London, UK. Academic Press. pp. 3-90.

Gooday, A. J., Jorissen, F., Levin, L. A., Middelburg, J. J., Naqvi, S. W. A., Rabalais, N. N., Zhang, J., 2009. Historical records of coastal eutrophication-induced hypoxia. Biogeosciences. 6 (8), 1707-1745.

Gréselle, B., Pittet, B., Mattioli, E., Joachimski, M., Barbarin, N., Riquier, L., Pucéat, E., 2011. The Valanginian isotope event: A complex suite of palaeoenvironmental perturbations. Palaeogeogr. Palaeoclimatol. Palaeoecol. 306(1-2), 41-57.

Hammer, O., Harper, D.A.T., Ryan, P.D., 2001. PAST: paleontological statistics software package for education and data analysis. Palaeontol Electronica. 4 (1), p4.

Hart, M. B., 1991. The Late Cenomanian calcisphere global bioevent. Proc Ussher Soc. 7 (4), 413-417.

Hart, M. B., Fitzpatrick, M. E. J., 1995. Kimmeridgian palaeoenvironments; a micropalaeontological perspective. Proc Ussher Soc. 8, 433-433.

Hinz, K., Krause, W., 1982. The continental margin of Queen Maud Land/Antarctica: Seismic sequences, structural elements and geological development. Reihe E. Geol. Jahrb. 23, 17-41.

Holbourn, A. E., Kaminski, M. A., 1994. Lower Cretaceous benthic foraminifera from DSDP and ODP sites of the Indian Ocean: a review and synthesis. In Microfossils and oceanic environments. Proceedings of the symposium on the ocean drilling program and the marine biosphere, Aberystwyth, Wales. pp. 77-90.

Holbourn, A. E., Kaminski, M. A., 1995a. Valanginian to Barremian benthic foraminifera from ODP site 766 (Leg 123, Indian ocean). Micropaleontology. 197-250.

816 Holbourn, A. E., Kaminski, M. A., 1995b. Lower Cretaceous benthic foraminifera from DSDP Site 263:
817 micropalaeontological constraints for the early evolution of the Indian Ocean. Mar. Micropaleontol.
818 26(1-4), 425-460.
819
820 Holbourn, A., Kuhnt, W., Erbacher, J., 2001a. Benthic foraminifers from lower Albian black shales (Site
821 1049, ODP Leg 171): evidence for a non “uniformitarian” record. J. Foraminiferal Res. 31(1), 60-74.
822
823 Holbourn, A., Kuhnt, W., Soeding, E., 2001b. Atlantic paleobathymetry, paleoproductivity and
824 paleocirculation in the late Albian: the benthic foraminiferal record. Palaeogeogr. Palaeoclimatol.
825 Palaeoecol. 170 (3-4), 171-196.
826
827 Jeremiah, J., 2001. A Lower Cretaceous nannofossil zonation for the North Sea Basin. J Micropalaeontol.
828 20(1), 45-80.
829
830 Jorissen, F. J., 1999. Benthic foraminiferal microhabitats below the sediment-water interface. In Modern
831 foraminifera. Springer, Dordrecht. pp. 161-179.
832
833 Jorissen, F. J., Destigter, H. C., Widmark, J. G. V., 1995, A conceptual model explaining benthic
834 foraminiferal microhabitats. Mar. Micropaleontol. 26, 3-15.
835
836 Jorissen, F. J., Fontanier, C., and Thomas, E., 2007, Paleoceanographical proxies based on deep-sea
837 benthic foraminiferal assemblage characteristics. Dev. Mar. Geol. 1, 263-325.
838
839 Kaiho, K., 1994. Benthic foraminiferal dissolved-oxygen index and dissolved-oxygen levels in the

modern ocean. Geology. 22 (8), 719-722.

Kaiho, K., Hasegawa, T., 1994. End-Cenomanian benthic foraminiferal extinctions and oceanic dysoxic events in the northwestern Pacific Ocean. Palaeogeogr. Palaeoclimatol. Palaeoecol. 111 (1-2), 29-43.

Kaminski, M. A., Boersma, E., Tyszka, J., Holbourn, A. E. L., 1995. Response of deep-water agglutinated foraminifera to dysoxic conditions in the California Borderland basins. Grzyb Found Spec Pub. 131-140.

Kessels, K., Mutterlose, J., & Michalzik, D., 2006. Early Cretaceous (Valanginian-Hauterivian) calcareous nannofossils and isotopes of the northern hemisphere: proxies for the understanding of Cretaceous climate. Lethaia. 39(2), 157-172.

Koch, M. C. Friedrich, O., 2012. Campanian-Maastrichtian intermediate- to deep-water changes in the high latitudes: Benthic foraminiferal evidence. Paleoceanography. 27, 1-11.

Koutsoukos, E. A. M., 1989. Mid-to Late Cretaceous microbiostratigraphy, palaeo-ecology and palaeogeography of the Sergipe Basin, northeastern Brazil. Ph.D. Thesis University of Plymouth. Plymouth, England. 471p.

Koutsoukos, E. A. M., Hart, M. B., 1990. Cretaceous foraminiferal morphogroup distribution patterns, palaeocommunities and trophic structures: a case study from the Sergipe Basin, Brazil. Earth and Environmental Science Transactions of the Royal Society of Edinburgh. 81 (03), 221-246.

Kouwenhoven, T. J., van der Zwaan, G. J., 2006. A reconstruction of late Miocene Mediterranean circulation patterns using benthic foraminifera. Palaeogeogr. Palaeoclimatol. Palaeoecol. 238, 373-385.

Kozdon, R., Kelly, D. C., Kitajima, K., Strickland, A., Fournelle, J. H., Valley, J. W., 2013, In situ $\delta^{18}O$ and Mg/Ca analyses of diagenetic and planktic foraminiferal calcite preserved in a deep-sea record of the Paleocene-Eocene thermal maximum: Paleoceanography. 28, 517-528.

Leckie, R. M., 1990. Middle Cretaceous planktonic foraminifers of the Antarctic margin: Hole 693A, ODP Leg 113. Proc Ocean Drill Prog Sci Results. 113, 319-324.

Littler, K., Robinson, S. A., Bown, P. R., Nederbragt, A. J., Pancost, R. D., 2011. High sea-surface temperatures during the Early Cretaceous Epoch. Nat. Geosci. 4 (3), 169.

Lowery, C. M., Corbett, M. J., Leckie, R. M., Watkins, D., Romero, A. M., Pramudito, A., 2014. Foraminiferal and nannofossil paleoecology and paleoceanography of the Cenomanian–Turonian Eagle Ford Shale of southern Texas. Palaeogeogr. Palaeoclimatol. Palaeoecol. 413, 49-65.

Løfaldli, M., Nagy, J., 1980. Foraminiferal stratigraphy of Jurassic deposits on Kongsøya, Svalbard. Norsk Polarinst. Skr. 172, 63-96.

Martinez M., Deconinck, J.-F., Pellenard, P., Riquier, L., Company M., Reboulet S., Moiroud, M., 2015. Astrochronology of the Valanginian–Hauterivian stages (Early Cretaceous): chronological relationships between the Paraná–Etendeka large igneous province and the Weissert and the Faraoni

events. Glob. Planet. Change. 131, 158-173.

Meissner, P., Mutterlose, J., Bodin, S., 2015. Latitudinal temperature trends in the northern hemisphere during the Early Cretaceous (Valanginian–Hauterivian). Palaeogeogr. Palaeoclimatol. Palaeoecol. 424, 17-39.

Möller, C., Mutterlose, J., Alsen, P., 2015. Integrated stratigraphy of Lower Cretaceous sediments (Ryazanian–Hauterivian) from North-East Greenland. Palaeogeogr. Palaeoclimatol. Palaeoecol. 437, 85-97.

Murray, J. W., 1991. Ecology and paleoecology of benthic foraminifera. Longman, Harlow. pp. 397.

Murray, J. W., Alve, E., 1999, Taphonomic experiments on marginal marine foraminiferal assemblages: How much ecological information is preserved? Palaeogeogr. Palaeoclimatol. Palaeoecol. 149, 183-197.

Mutterlose, J., Wise Jr, S. W., 1990. Lower Cretaceous nannofossil biostratigraphy of ODP Leg 113 holes 692b and 693a, continental slope off east Antarctica, Weddell Sea. Proc Ocean Drill Prog Sci Results. 113, 325-353.

Nyong, E. E., Olsson, R. K., 1984. A paleoslope model of Campanian to Lower Maestrichtian foraminifera in the North American basin and adjacent continental margin. Mar. Micropaleontol. 8 (6), 437-477.

O'Brien, C. L., Robinson, S. A., Pancost, R. D., Damste, J. S. S., Schouten, S., Lunt, D. J., Wrobel, N. E., 2017. Cretaceous sea-surface temperature evolution: Constraints from TEX_{86} and planktonic foraminiferal oxygen isotopes. Earth-Sci. Rev. 172, 224-247.

O'Connell, S. B., 1990. Sedimentary facies and depositional environment of the Lower Cretaceous East Antarctic margin: sites 692 and 693. Proc Ocean Drill Prog Sci Results. 113, 71-88.

Owen, H. G., 1983. Atlas of continental displacement, 200 million years to the present. Cambridge University Press. England. pp. 170.

Racki, G., Cordey, F., 2000. Radiolarian palaeoecology and radiolarites: is the present the key to the past? Earth-Sci. Rev. 52(1-3), 83-120.

Reolid, M., 2020. Microfossil assemblages and geochemistry for interpreting the incidence of the Jenkyns Event (early Toarcian) in the south-eastern Iberian Palaeomargin (External Subbetic, SE Spain). J. Micropalaeontology. 39(2), 233-258.

Reolid, M., Martínez-Ruiz, F., 2012. Comparison of benthic foraminifera and geochemical proxies in shelf deposits from the Upper Jurassic of the Prebetic (southern Spain). J. Iber. Geol. 38(2), 449-465.

Reolid, M., Rodríguez-Tovar, F. J., Nagy, J., Olóriz, F., 2008. Benthic foraminiferal morphogroups of mid to outer shelf environments of the Late Jurassic (Prebetic Zone, southern Spain): characterization of biofacies and environmental significance. Palaeogeogr. Palaeoclimatol. Palaeoecol. 261 (3-4), 280-

299.

Reolid, M., Chakiri, S., Bejjaji, Z., 2013. Adaptative strategies of the Toarcian benthic foraminiferal assemblages from the Middle Atlas (Morocco): palaeoecological implications. J. Afr. Earth Sci. 84, 1-12.

Reolid, M., Sánchez-Quiñónez, C. A., Alegret, L., Molina, E., 2015. Palaeoenvironmental turnover across the Cenomanian-Turonian transition in Oued Bahloul, Tunisia: foraminifera and geochemical proxies. Palaeogeogr. Palaeoclimatol. Palaeoecol. 417, 491-510.

Reolid, M., Duarte, L. V., Rita, P., 2019. Changes in foraminiferal assemblages and environmental conditions during the T-OAE (Early Jurassic) in the northern Lusitanian Basin, Portugal. Palaeogeogr. Palaeoclimatol. Palaeoecol. 520, 30-43.

Riccardi, A. C., 1988. The Cretaceous system of southern south America (Vol. 168). Geological Society of America. 161p.

Riegraf, W., 1989. Benthonische Schelf-Foraminiferen aus dem Valanginium-Hauterivium (Unterkreide) des Indischen Ozeans südwestlich Madagaskar (Deep Sea Drilling Project Leg 25, Site 249). Geol Rundsch. 78 (3), 1047-1061.

Robert, C., Maillot, H., 1990. Paleoenvironments in the Weddle Sea area and Antarctic climates, as deduced from clay mineral associations and geochemical data, ODP Leg 113. Proc Ocean Drill Prog Sci Results. 113, 51-70.

Rohling, E. J., Jorissen, F. J., De Stigter, H. C., 1997. 200 year interruption of Holocene sapropel formation in the Adriatic Sea. J. Micropalaeontol. 16(2), 97-108.

Rohling, E., Mayewski, P., Abu-Zied, R., Casford, J., Hayes, A., 2002. Holocene atmosphere-ocean interactions: records from Greenland and the Aegean Sea. Clim. Dyn. 18(7), 587-593.

Roth, P. H., 1983. Jurassic and Lower Cretaceous calcareous nannofossils in the western North Atlantic (Site 534): biostratigraphy, preservation, and some observations on biogeography and palaeoceanography. In: Sheridan, R.E., Gradstein, F.M. (Eds.), Init. Reports DSDP 76. Init. Rep. Deep Sea Drill. Proj. 587-621.

Royer, D. L., Berner, R. A., Park, J., 2007. Climate sensitivity constrained by CO_2 concentrations over the past 420 million years. Nature. 446(7135), 530-532.

Rykaczewski, R. R., Dunne, J. P., Sydeman, W. J., García-Reyes, M., Black, B. A., Bograd, S. J., 2015.Pole ward intensification of coastal upwelling in response to global warming. Geophys. Res. Lett. 42, 6424-6431.

Scheibnerová, V., 1976. Cretaceous foraminifera of the Great Australian Basin. Mem. Geol. Surv. N.S.W. 17, 1-265.

Scheibnerová, V., 1973. A comparison of the austral and boreal Lower Cretaceous foraminiferal and ostracodal assemblages. In Proceedings of the international symposium on the boreal lower cretaceous

(1972). Seel House, Liverpool. pp. 407-414.

Schlanger, S. O., Jenkyns, H. C., 1976. Cretaceous oceanic anoxic events: causes and consequences. Geol Mijnbouw. 55, 179-184.

Schmiedl, G., Hemleben, C., Keller, J., Segl, M., 1998. Impact of climatic changes on the benthic foraminiferal fauna in the Ionian Sea during the last 330,000 years. Paleoceanography. 13, 447-458.

Schmiedl, G., Mitschele, A., Beck, S., Emeis, K. C., Hemleben, C., Schulz, H., Weldeab, S., 2003. Benthic foraminiferal record of ecosystem variability in the eastern Mediterranean Sea during times of sapropel S5 and S6 deposition. Palaeogeogr. Palaeoclimatol. Palaeoecol. 190, 139-164.

Schnack, K., 2000. Biostratigraphie und fazielle Entwicklung in der Oberkreide und im Alttertiär im Bereich der Kharga Schwelle, Westliche Wüste, southwest Ägypten: Ph.D. Thesis Nr. 151, Universität Bremen, Bremen. 142 p.

Scholle, P. A., Wenkam, C. R., 1982. Geological studies of the COST Nos. G-1 and G-2 wells, United States North Atlantic Outer Continental Shelf: Introduction. Geological. Studies of the cost Nos. G-1 and G-2 Wells, US North Atlantic Outer Continental Shelf. p. 194.

Scotese, C. R., 2014. Atlas of Early Cretaceous Paleogeographic Maps, Paleomap Atlas for ArcGIS, volume 2, The Cretaceous, Maps 23-31, Mollweide Projection, Paleomap Project, Evanston, IL. DOI. 10.13140/2.1.4099.4560.

1008 Sen Gupta, B. K., Machain-Castillo, M. L., 1993. Benthic foraminifera in oxygen poor habitats. Mar.
1009 Micropaleontol. 20, 183-201.
1010
1011 Sewall, J. V., Van De Wal, R. S. W., van Der Zwan, K., Van Oosterhout, C., Dijkstra, H. A., Scotese, C.
1012 R., 2007. Climate model boundary conditions for four Cretaceous time slices. Clim. Past. 3(4), 647-
1013 657.
1014
1015 Shannon, C. E., Weaver, W., 1949. The Mathematical Theory of Communication. University of Illinois
1016 Press, Urbana, p. 125.
1017
1018 Sprovieri, M., Coccioni, R., Lirer, F., Pelosi, N., Lozar, F., 2006. Orbital tuning of a lower Cretaceous
1019 composite record (Maiolica Formation, central Italy). Paleoceanography. 21(4), 1-19.
1020
1021 Thiede, D.S., Vasconcelos, P.M., 2010. Paraná flood basalts: rapid extrusion hypothesis confirmed by
1022 new 40Ar/39Ar results. Geology, 38(8), 747-750.
1023
1024 Thierstein, H. R., 1976. Mesozoic calcareous nannoplankton biostratigraphy of marine sediments. Mar.
1025 Micropaleontol. 1, 325-362.
1026
1027 Tyszka, J., 1994. Response of Middle Jurassic benthic foraminiferal morphogroups to dysoxic/anoxic
1028 conditions in the Pieniny Klippen Basin, Polish Carpathians. Palaeogeogr. Palaeoclimatol. Palaeoecol.
1029 110 (1-2), 55-81.
1030
1031 van der Zwaan, G. J., Duijnstee, I. A. P., Den Dulk, M., Ernst, S. R., Jannink, N. T., Kouwenhoven, T. J.,

1032 1999. Benthic foraminifers: proxies or problems? a review of paleocological concepts. Earth-Sci. Rev.
1033 46 (1-4), 213-236.
1034
1035 van Morkhoven, F. P., Berggren, W. A., Edwards, A. S., Oertli, H. J., 1986, Cenozoic cosmopolitan deep-
1036 water benthic foraminifera: Bulletin des Centres de Recherches Exploration-Production Elf-
1037 Aquitaine, Pau. 421 p.
1038
1039 Wahyudi, W., Minagawa, M., 2013. The Last 41.000 Years Fluctuation in Atmosperic CO2 Concentration
1040 Inferred from The Changes in Oxygen and Carbon Stable Isotopes Ratios of The Marine Sediment.
1041 Eksplorium. 33 (1), 15-24.
1042
1043 Weissert H., 1989. C-isotope stratigraphy, a monitor of paleoenvironmental change: a case study from
1044 the early Cretaceous. Surv. Geophys. 10(1), 1-61.
1045
1046 Weissert, H., Erba, E., 2004. Volcanism, CO_2 and palaeoclimate: a Late Jurassic–Early Cretaceous carbon
1047 and oxygen isotope record. J. Geol. Soc. Lond. 161, 695-702.
1048
1049 Westermann, S., Föllmi, K. B., Adatte, T., Matera, V., Schnyder, J., Fleitmann, D., Duchamp-Alphonse,
1050 S., 2010. The Valanginian $\delta^{13}C$ excursion may not be an expression of a global oceanic anoxic event.
1051 Earth Planet Sci Lett. 290(1-2), 118-131.
1052
1053 Wignall, P., Newton, R., 1998. Pyrite framboid diameter as a measure of oxygen deficiency in ancient
1054 mudrocks. Am. J. Sci. 298, 537-552.
1055

Wilford, G. E., Brown, P. J., 1994. Maps of late Mesozoic-Cenozoic Gondwana break-up: some palaeogeographical implications. History of the Australian vegetation: Cretaceous to Recent. Edited by Robert S. Hill, University of Adelaide Press, South Australia, 5-13.

Zinsmeister, W. J., 1987. Cretaceous paleogeography of Antarctica. Palaeogeogr. Palaeoclimatol. Palaeoecol. 59, 197-206.

Appendix. Taxonomic appendix

The list of benthic foraminifera cited in the text are based on the works by Ellis and Messina (1940-2015), Riergraf (1989), and Holbourn and Kaminski (1995a, b).

Citharina d'Orbigny, 1839

Laevidentalina Loeblich & Tappan, 1986

- *Laevidentalina debilis* (Hantken) = *Dentalina debilis* Hantken, 1868
- *Laevidentalina distincta* (Reuss) = *Dentalina distincta* Reuss, 1868
- *Laevidentalina guttifera* (d'Orbigny) = *Dentalina guttifera* d'Orbigny, 1846
- *Laevidentalina soluta* (Reuss) = *Dentalina soluta* Reuss, 1851

Globulina prisca Reuss, 1863

Lagena Reuss, 1863

- *Lagena sulcata* (Walker & Jacob, 1798)
- *Lagena ovata* (Terquem, 1858)

Lenticulina Lamarck, 1804

- *Lenticulina lideri* Romanova, 1960
- *Lenticulina involvens* (Wiśniowski, 1890)
- *Lenticulina pulchella* (Reuss, 1863)
- *Lenticulina turgidula* (Reuss, 1863)

Marginulina d'Orbigny, 1826

- *Marginulina bullata* Reuss, 1845
- *Marginulina gatesi* Tappan, 1957

Nodosaria sceptrum Reuss, 1863

Planularia complanata (Reuss, 1845)

Saracenaria Defrance, 1824

Saracenaria bronni (Roemer, 1841)

Saracenaria tsaramandrosoensis Espitalié & Sigal, 1963

Vaginulinopsis Silvestri, 1904

Vaginulinopsis enodis Loeblich & Tappan, 1950

Vaginulinopsis excentrica Cornuel, 1848

Figures

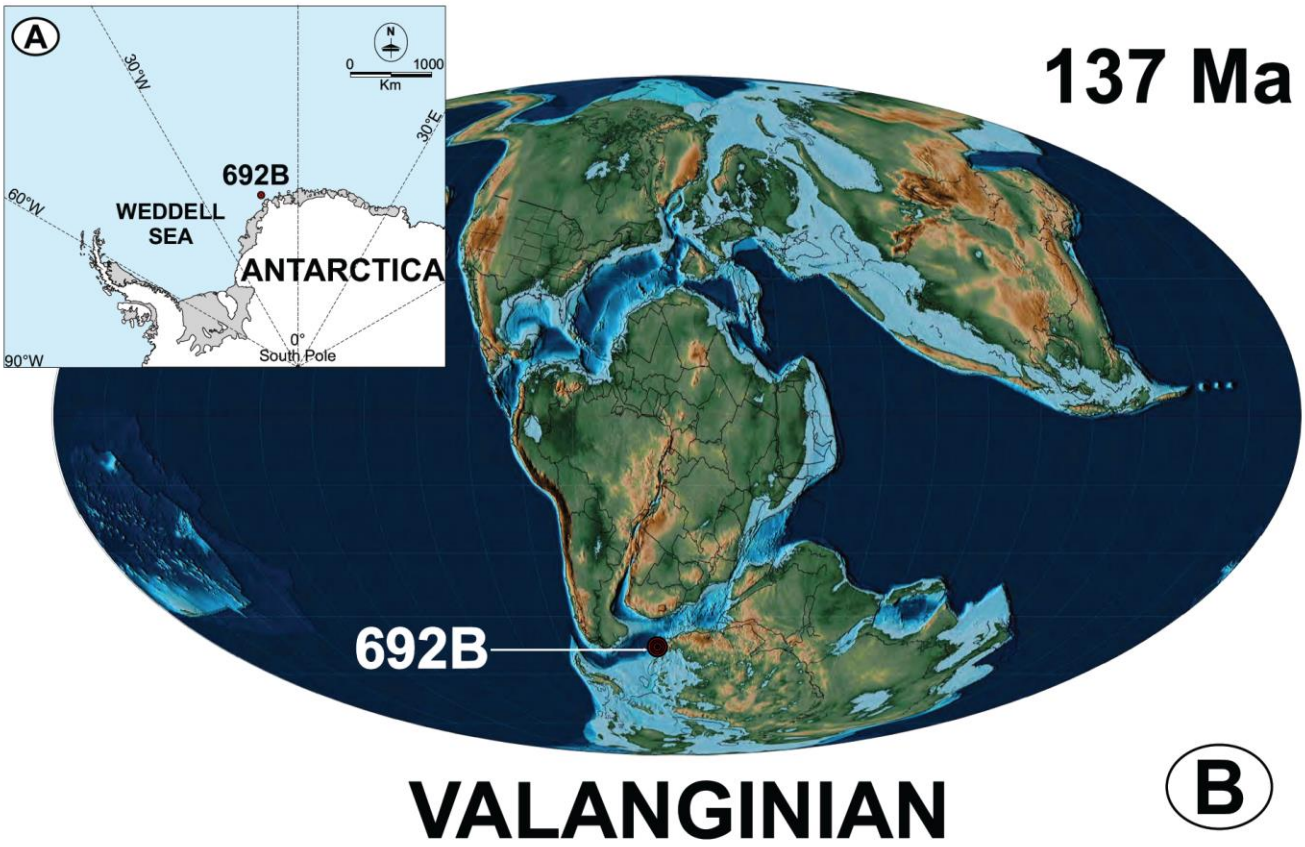

Fig 1. A. Location of ODP Hole 692B in the Weddell Sea, Antarctica. **B.** Paleogeographic reconstruction of the Gondwana continent during the Valanginian (137 Ma), showing the position of ODP Hole 692B along the Antarctica margin (modified from Scotese, 2014).

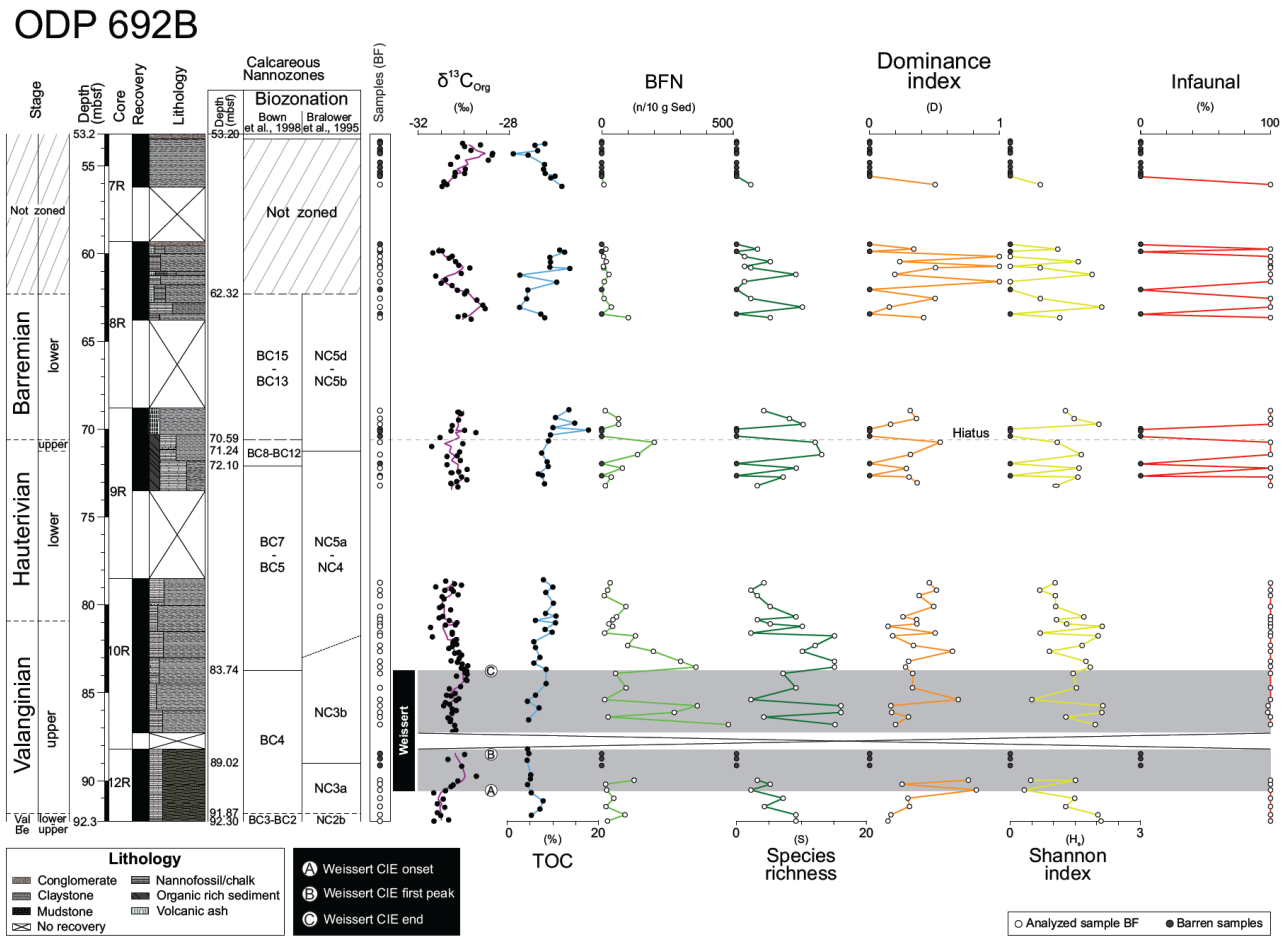

Fig. 2. Lithological, geochemical, and benthic foraminiferal assemblage data from ODP Hole 692B: benthic foraminiferal numbers (BFN), species richness (S), dominance (D), Shannon Index (Hs), and infaunal morphogroup of benthic foraminifera. Lithology according to Barker et al. (1988). Age and calcareous nannofossils biozonation from this study and Cavalheiro et al. (2021). Organic carbon isotopes ($\delta^{13}C_{org}$), total organic carbon (TOC), the position of the Weissert Event (grey band) and peaks A, B, C are according to Cavalheiro et al. (2021).

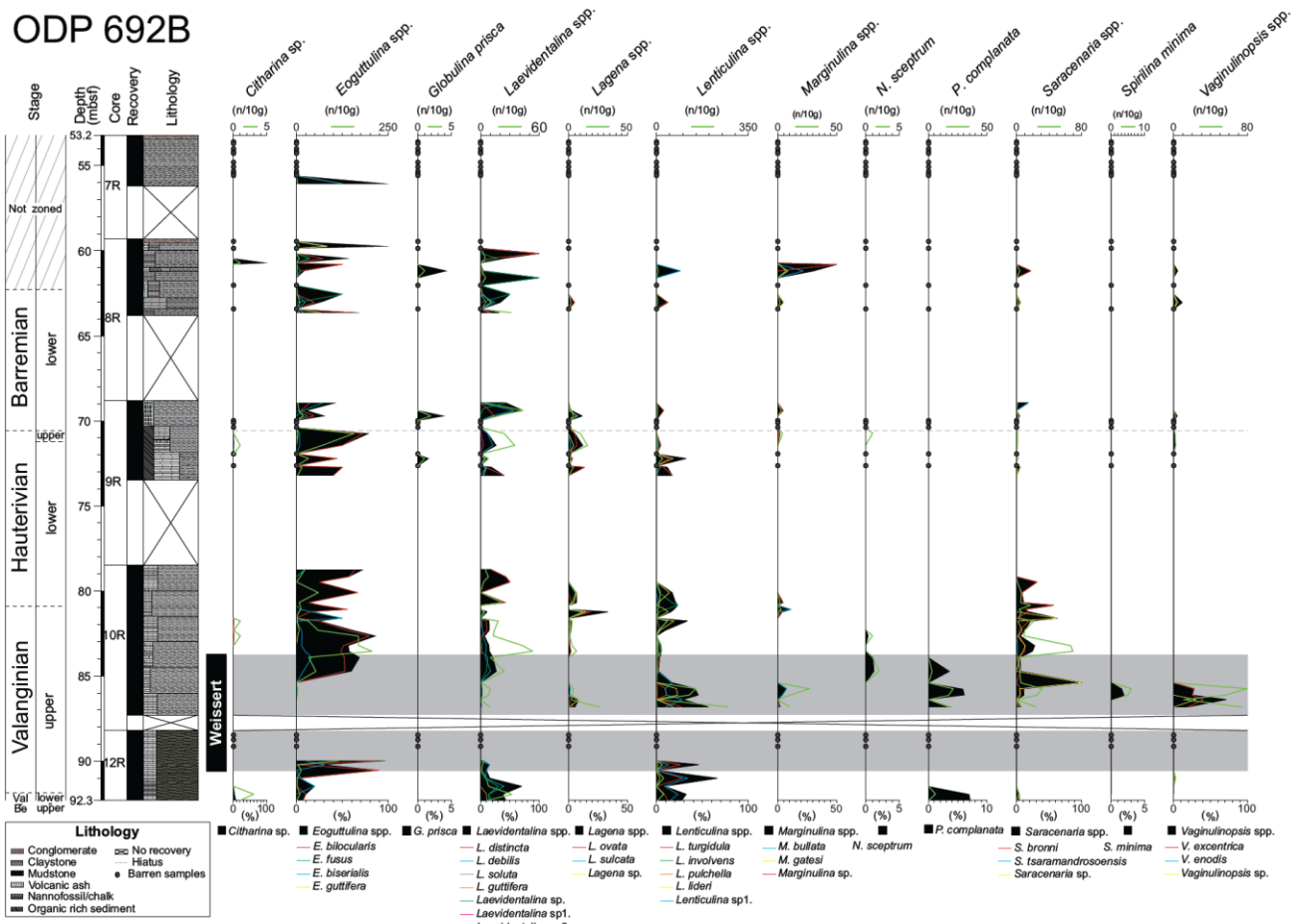

Fig. 3. Absolute and relative abundances of the most important benthic foraminiferal taxa in ODP Hole 692B. Lithology according to Barker et al. (1988).

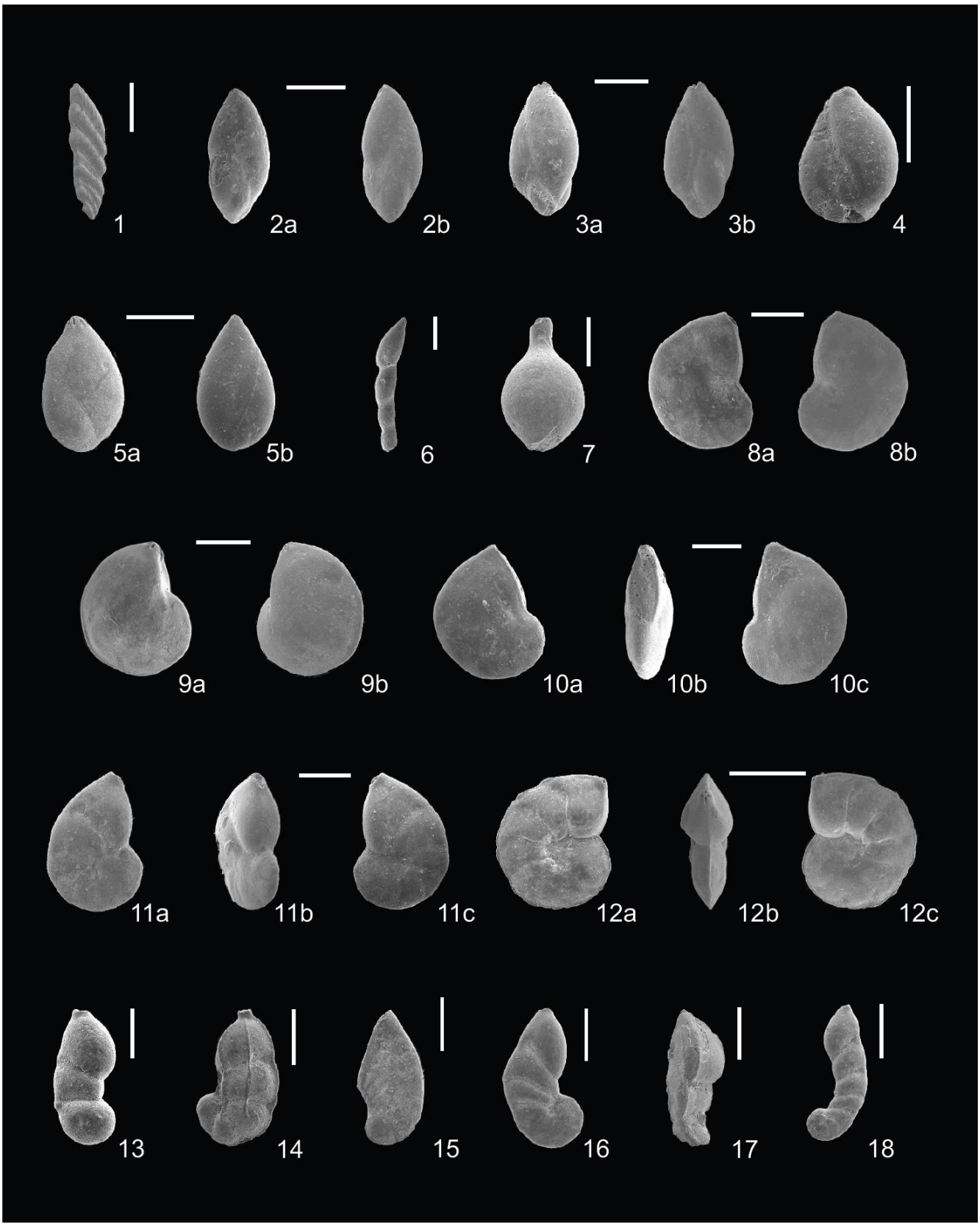

1163

1164 **Fig. 4.** Benthic foraminifera from the Lower Cretaceous in ODP Hole 692B organized according to

genera. Scale-bars are 100 μm.

1. *Citharina* sp. (113-692B-12R-3, 112-115 cm). 2. a/b *Eoguttulina bilocularis* (113-692B-8R-3, 75-78 cm). 3. a/b *Eoguttulina fusus* (113-692B-9R-2, 10-13 cm). 4. *Eoguttulina guttifera* (113-692B-9R-2, 45-48 cm). 5. a/b *Globulina prisca* (113-692B-9R-3, 42-45 cm). 6. *Laevidentalina debilis* (113-692B-9R-1, 60-63 cm). 7. *Lagena ovata* (113-692B-9R-1, 60-63 cm). 8. a/b *Lenticulina involvens* (113-692B-10R-3, 27-30 cm). 9. a/b *Lenticulina lideri* (113-692B-9R-3, 42-45 cm). 10. a/b/c *Lenticulina pulchella* (113-692-10R-6, 13-16 cm). 11. a/b/c *Lenticulina turgidula* (113-692B-10R-6, 82-85 cm). 12. a/b/c *Lenticulina* sp. 1. (113-692B-10R-6, 82-85 cm). 13. *Marginulina bullata* (113-692B-9R2, 45-48 cm). 14. *Marginulina gatesi* (113-692B-8R-3, 75-78 cm). 15. *Planularia complanata* (113-692B-10R-6, 82-85 cm). 16. *Saracenaria bronni* (113-692B-10R-3, 27-30 cm). 17. *Saracenaria tsaramandrosoensis* (113-692B-10R-6, 39-42 cm). 18. *Vaginulinopsis enodis* (113-692B-9R-2, 115-117.5 cm).

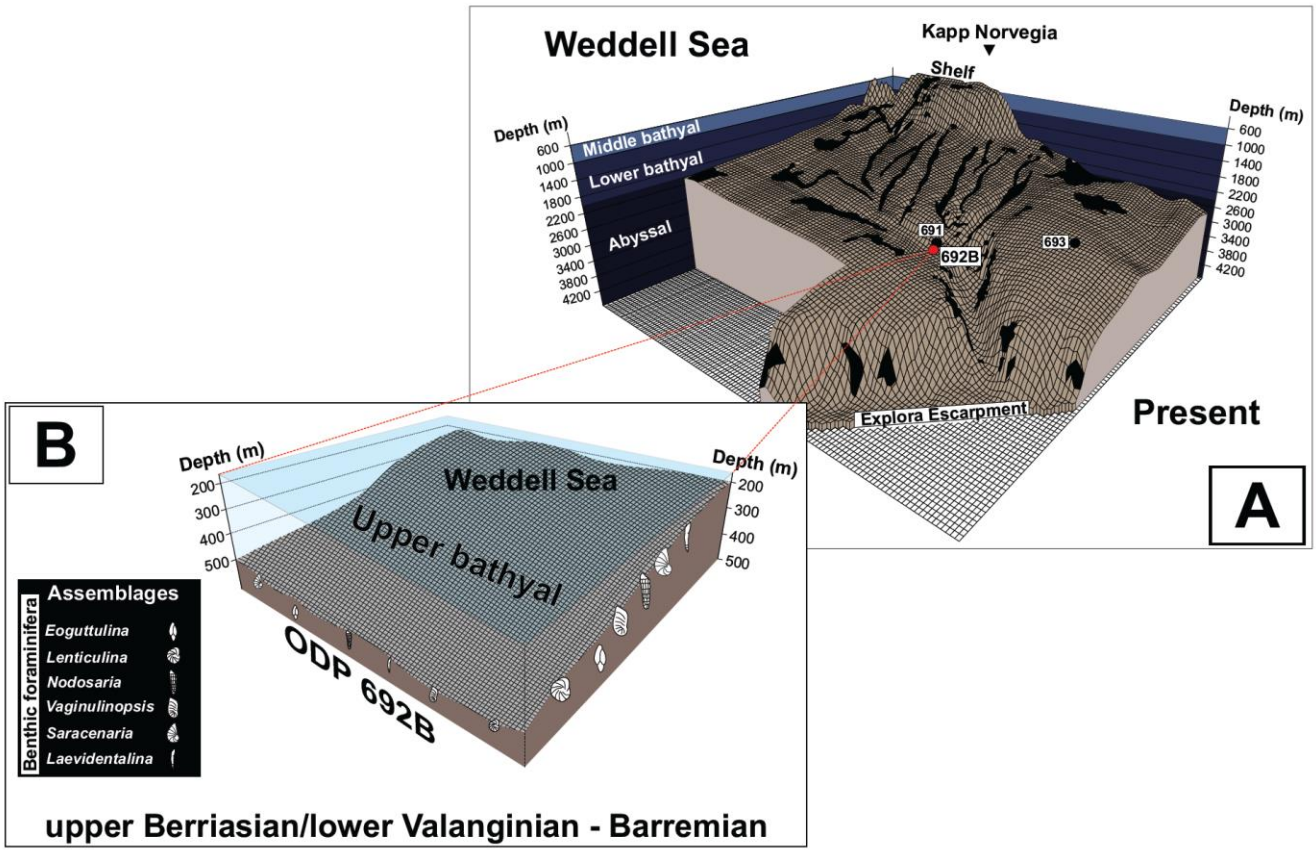

Fig. 5. A. Present bathymetry of the Antarctic continental margin and the Wegener Canyon (modified after Fütterer et al., 1990). **B.** Paleobathymetric reconstruction of ODP Hole 692B during the Lower Cretaceous based on the occurrence of benthic foraminiferal assemblages that indicate an outer neritic - upper bathyal environment (see text for further explanation).

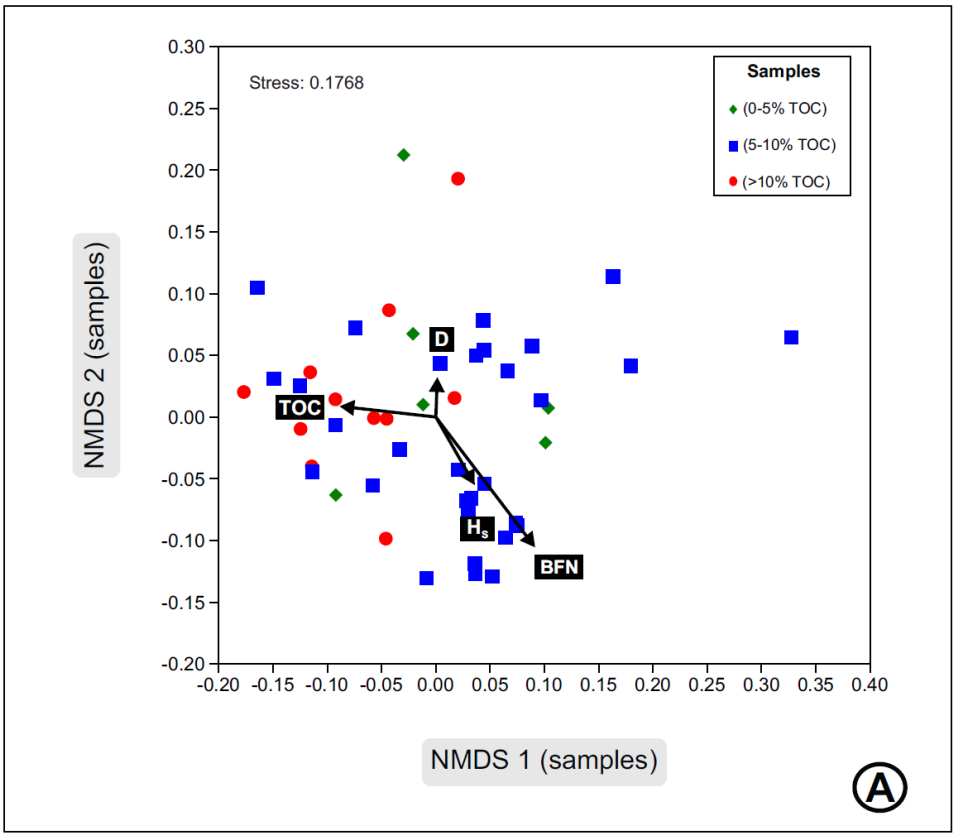
Stress: 0.1768
Samples
(0-5% TOC)
(5-10% TOC)
(>10% TOC)
NMDS 2 (samples)
NMDS 1 (samples)
D
TOC
Hs
BFN
A

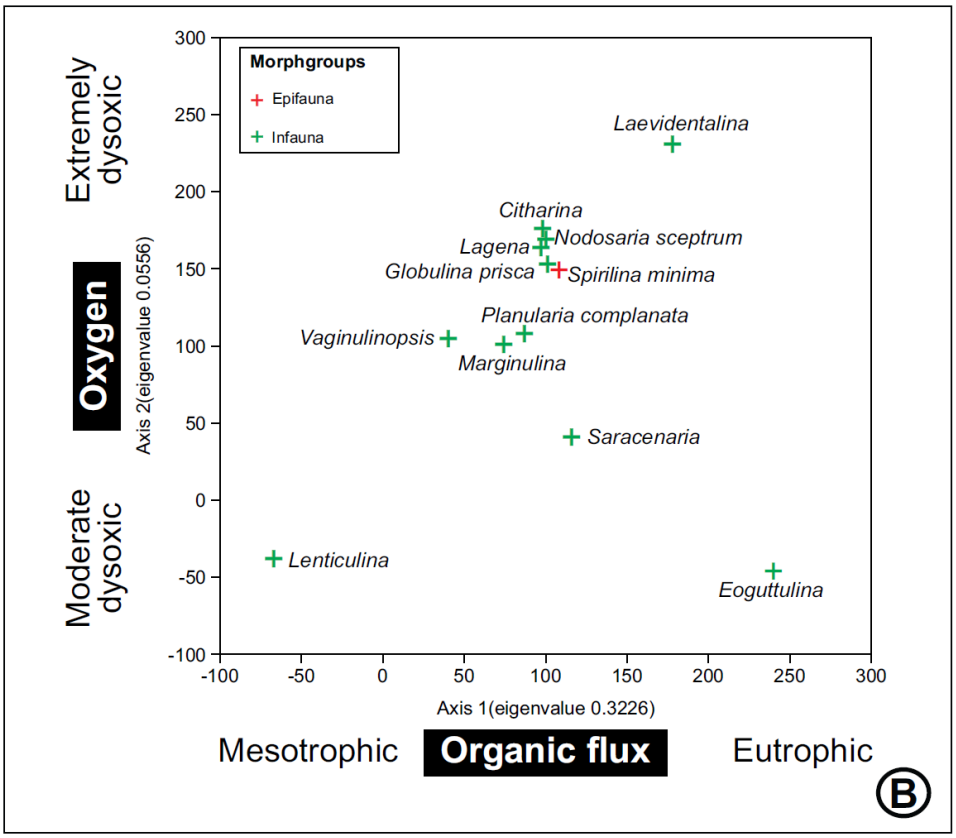
Morphgroups
Epifauna
Infauna
Extremely dysoxic
Oxygen
Moderate dysoxic
Axis 2(eigenvalue 0.0556)
Axis 1(eigenvalue 0.3226)
Laevidentalina
Citharina
Lagena
Nodosaria sceptrum
Globulina prisca
Spirilina minima
Planularia complanata
Vaginulinopsis
Marginulina
Saracenaria
Lenticulina
Eoguttulina
Mesotrophic
Organic flux
Eutrophic
B

1199

Fig. 6. Multivariate analyses of benthic foraminiferal assemblages in ODP Hole 692B. **A.** Non-Metric Multidimensional Scaling (NMDS: Q-mode) showing a relationship between the TOC content and the benthic foraminiferal parameters: benthic foraminifera numbers (BFN) and diversity indices (D: Dominance index and H_S: Shannon index). From fitted environmental vectors, the TOC content and the BFN are related to the NMDS axis 1, which is controlled by benthic foraminiferal assemblages. Samples with high TOC values (left side) and D (right side) show the opposite similarity to those with high BFN and H_S values. **B.** Detrended Correspondence Analyses (DCA: R-mode) of benthic foraminiferal abundances of Hole 692B. The first axis (eigenvalue 0.3226) is associated with the organic carbon flux, while the second axis (eigenvalue 0.0556) is linked to oxygen depletion (see text for further explanation).

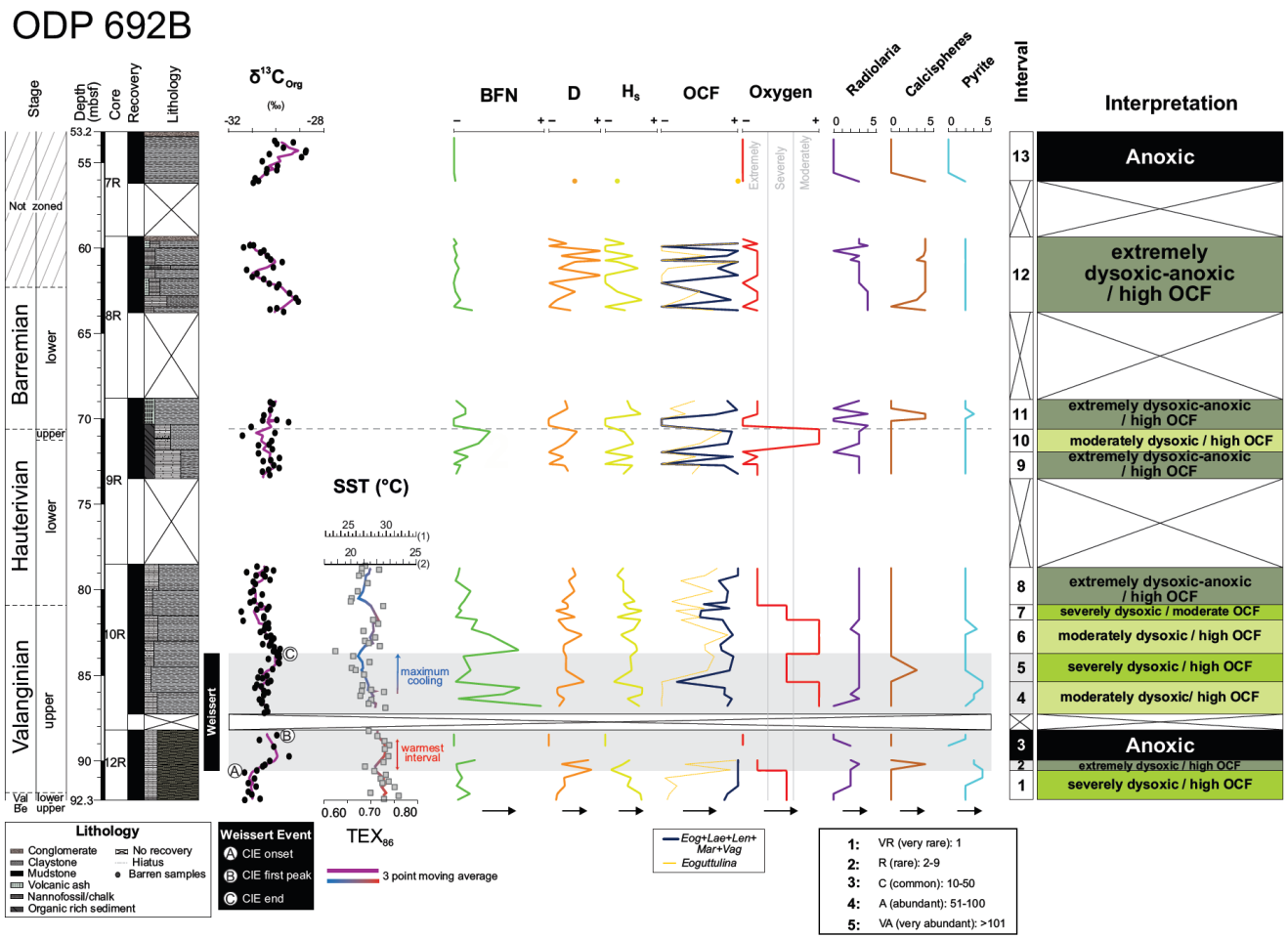

Fig. 7. Paleoceanographic reconstruction of bottom-water conditions in ODP Hole 692B is based on the abundances and composition of the benthic foraminiferal assemblages during the Lower Cretaceous. Changes in organic carbon fluxes (OCF) gained from the abundance of diagnostic benthic foraminiferal taxa (Eogu: *Eoguttulina*; Laev: *Laevidentalina*; Lent: *Lenticulina*; Mar: *Marginulina*; Vag: *Vaginulinopsis*) and oxygen estimations derived from BFN, diversity indices (D - Hs), palaeoecological preferences of each taxon, and statistical analyses (NMDS and DCA) (see text for further explanation). Thirteen intervals have been identified as follows: I) upper Berriasian - lower Valanginian (interval 1); upper Valanginian (intervals 1 to 7), II) Hauterivian (intervals 8, 9 and 10), and III) Barremian and post-Barremian (intervals 11, 12 and 13). Radiolaria, calcispheres, and pyrite abundances from this study (Supplementary data, Table S1). Organic carbon isotopes ($\delta^{13}C_{org}$), the position of the Weissert Event

(grey band) and peaks A (CIE onset), B (CIE first peak), and C (CIE end) are according to Cavalheiro et al. (2021). Sea surface temperatures (SSTs) from TEX_{86} paleothermometry (red curve: warmer values; blue curve: colder values) showing the calibration in degree °C (1: Bayspar and 2: restricted basin calibrations) are according to Cavalheiro et al. (2021).

TABLE

Benthic foraminifera	Morphogroups		Oxygen			Organic matter			Paleodepth						References
	Epifauna	Infauna	Low	Middle	High	Low	Middle	High	IN	50 m	MN	100	ON	200	UB	500	MB	1000	LB	2000	
Citharina	X	X																			5, 14, 22
Eoguttulina		X																			2, 5, 6, 11, 25, 29
Globulina	X	X																			5, 8, 14, 17
Laevidentalina	X	X																			8, 10, 14, 16, 17, 20, 21, 24, 27
Lagena	X	X																			5, 8, 9, 14, 17, 22
Lenticulina	X	X																			4, 5, 7, 8, 9, 12, 13, 14, 15, 16, 17, 18, 19, 21, 22, 27, 28, 29
Marginulina	X	X																			5, 8, 13, 14, 25, 26
Nodosaria	X	X																			3, 4, 5, 8, 14, 18, 21, 24
Planularia	X	X																			5, 8, 14, 21, 27
Saracenaria	X	X																			5, 7, 8, 12, 14, 17
Spirillina	X																				5, 8, 14, 21, 22, 23
Vaginulinopsis	X	X																			1, 6, 12, 13

Table 1. Paleoecological preferences of the benthic foraminifera according to the morphogroups identified by Corliss and Chen (1988). Paleoecological and paleobathymetric interpretation are based on different studies: Løfaldli and Nagy, (1980)[1]; Scholle and Wenkam, (1982)[2]; Nyong and Olson, (1984)[3]; De Azevedo, (1987)[4]; Koutsoukos, (1989)[5]; Riegraf, (1989)[6]; Koutsoukos and Hart, (1990)[7]; Tyszka, (1994)[8]; Kaiho, (1994)[9]; Kahio and Hasegawa, (1994)[10]; Hart and Fitzpatrick, (1995)[11]; Holbourn and Kaminski, (1995a)[12]; Decker and Rögl, (1998)[13]; Frenzel, (2000)[14]; Schnack, (2000)[15]; Holbourn et al. (2001b)[16]; Alegret et al. (2003)[17]; Kouwnhoven and van der Zwann, (2006)[18]; Friedrich et al. (2006)[19]; Friedrich and Erbacher, (2006)[20]; Reolid et al. (2008)[21]; Cetean et al. (2011)[22]; Reolid and Martinez-Ruiz, (2012)[23]; Koch and Friedrich, (2012)[24]; Reolid et al. (2013)[25], Reolid et al. (2015)[26]; Aschckenazi-Polivoda et al. (2018)[27]; Giraldo-Gómez et al. (2018)[28]; Reolid et al. (2019)[29].

Supplementary data

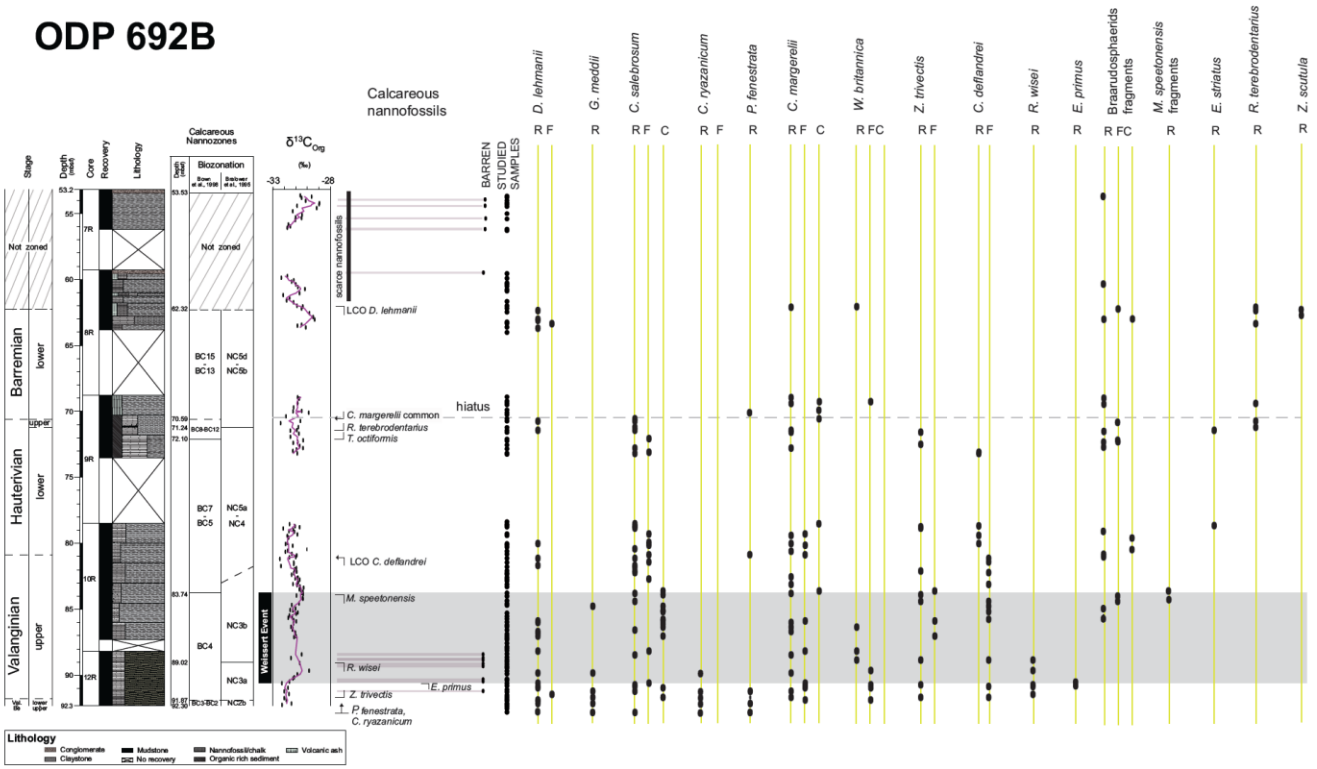

Supplementary data, Figure S1. Calcareous nannofossil zonations include the BC Zones for higher latitudes (Bown et al., 1998) and the NC Zones for lower latitudes (Bralower et al., 1995). On the right, the relative abundance of nannofossil species relevant for biostratigraphy is reported. R = Rare, 1 specimen in >30 fields of view; F = Frequent, 1 specimen in 11-30 fields of view; C = Common, 1 specimen in 2-10 fields of view. LCO (Last Common Occurrence). The dark grey lines correspond to samples barren of nannofossils. The carbon isotope curve is from Cavalheiro et al. (2021). The grey band corresponds to the Weissert Event interval.

Bown, P. R., Rutledge, D.C., Crux, J. A. Gallagher, L. T., 1998. Early Cretaceous. In *Calcareous Nannofossil Biostratigraphy* (ed Bown, P.R.) Chapman and Hall, Cambridge, 86-131.

Bralower, T. J., Leckie, R. M., Sliter, W. V., Thierstein, H. R., 1995. An integrated Cretaceous microfossil biostratigraphy. In *Geochronology, Time Scales and Global Stratigraphic Correlation* (eds Berggren

W.A., Kent D.V., Aubry M.-P. & Hardenbol J.) Spec. Publ. Soc. Econ. Paleontol. Mineral. **54**, 65-79.

Cavalheiro. L., Wagner, T., Steinig, S., Bottini, C., Dummann, W., Esegbue, O., Gambacorta, G., Giraldo-Gómez, V., Farnsworth, A., Flögel, S., Hofmann, P., Lunt, D., Rethemeyer, J., Torricelli, S., Erba, E., 2021. Impact of global cooling on Early Cretaceous high pCO_2 world during the Weissert Event. Nat. Commun. 12(1), 1-11.

Supplementary data, Table S1. Distribution chart of calcareous nannofossil in ODP Hole 692B.

Supplementary data, Table S2. Distribution chart of benthic foraminifera, radiolaria, calcispheres and pyrite in ODP Hole 692B.